

Neshat Zahraie

Study of Solvent Extraction for Metal Recovery during Lithium-Ion Batteries (LIBs) Recycling Process.

March 2021



Norwegian University of
Science and Technology

Study of Solvent Extraction for Metal Recovery during Lithium-Ion Batteries (LIBs) Recycling Process.

Neshat Zahraie

Material Science and Engineering

Submission date: March 2021

Supervisor: Dr. Christian Rosenkilde

Co-supervisor: Prof. Sulalit Bandyopadhyay

Norwegian University of Science and Technology
Department of Materials Science and Engineering

Abstract

Nowadays, the demand for electric vehicles (EVs) is rising, leading to an increase in the production of lithium-ion batteries (LIBs) since these batteries are used in EVs. A large number of Ni, Mn, Co, and Li resources are needed for the future production of LIBs, and this leads to future critical supply risks. The increasing demand for EVs will consequently represent a significant challenge regarding their status after reaching the end-of-life. The large amounts of spent LIBs need to be recycled effectively to minimize the environmental impact and help the industries move towards sustainable supply chains.

This thesis aims to study the extraction behavior of transition metals such as Mn from the leachates of spent LIBs using acidic extractant Bis (2-Ethylhexyl) phosphate (D2EHPA). The effect of equilibrium pH, extractant concentration, and initial concentration of metal ions on extraction efficiency were investigated. It was found that Mn can be selectively extracted from the leachates by D2EHPA with limited co-extraction of Co, Ni, and Li. With 10 vol% D2EHPA at the equilibrium pH of 3.5 and O/A=1, close to 90% of manganese was extracted with less than 7% co-extraction of Ni, Co, and Li. Although some Cu and Al were co-extracted with the Mn (low concentrations of Cu and Al, < 130 pm in the organic phase), these impurities can be eliminated with a proper scrubbing stage.

Furthermore, the extraction mechanism of Li from wastewater of spent LIBs wet-crushing step, by the combination of acidic (chelating) and neutral extractant was investigated. The β -diketone extraction system used in the experiment was composed of benzoyltrifluoroacetone (HBTA), trioctylphosphine oxide (TOPO), and kerosene. Lithium was extracted from wastewater by the β -diketone system with an extraction efficiency of 93% and higher. It can be concluded that the β -diketone system is suitable for Li recovery from wastewater streams of LIB recycling.

Preface

This master thesis is written on behalf of the environment and reactor technology group at the Department of Chemical Engineering, NTNU. The work has been performed between September 2020 and March 2021.

First of all, I would like to thank my supervisors Dr. Christian Rosenkilde and Prof. Sulalit Bandyopadhyay, for their wise advice, guidance, and support throughout this project. Thanks to the administrative and technical staff at the Department of Chemical Engineering at NTNU, the hardworking lab engineers that create a great working environment. Thanks to Jose Paulino Peris Sastre for giving the training for MP-AES, proofreading my report, and for being a good friend throughout the year that we worked together. Thanks to Stina Laugen for providing helpful comments on my report and helping me to improve my writing. Thanks to Tryanti Melinda Sinambela for providing mental support throughout the project. Finally, I would like to thank my friends (Siri, Amir, and Farnoush) and my family for the love, support, and encouragement.

I hereby declare that this is an independent work according to the Norwegian University of Science and Technology exam regulations.

Neshat Zahraie

Trondheim, 07.03.2021

Table of Contents

1	Introduction	1
1.1	An overview on lithium-ion battery recycling.....	4
1.2	Goals and Motivation.....	6
1.3	Thesis Outline	7
2	Theory and Literature Review:.....	8
2.1	Leaching:.....	8
2.2	Solvent Extraction Fundamentals:	9
2.2.1	Extractant Mechanisms:.....	10
2.2.2	Additives in Solvent System:.....	14
2.2.3	Thermodynamics of Solvent Extraction:	14
2.2.4	Saponification of Organic Phase.....	15
2.3	Reviews and Previous Studies.....	16
3	Experimental Procedure and Methodology:	22
3.1	Materials:.....	22
3.1.1	Chemical Reagents:	22
3.1.2	Experimental Set-Up:.....	22
3.2	Characterization Equipment:.....	27
3.2.1	X-ray Fluorescence Spectroscopy (XRF):.....	27
3.2.2	Microwave Plasma-Atomic Emission Spectrometer (MP-AES):.....	28
3.3	Methodology:	29
3.3.1	X-ray Fluorescence (XRF):.....	29
3.3.2	Microwave Plasma-Atomic Emission Spectrometer (MP-AES):.....	30
3.3.3	Solvent Extraction.....	31
4	Results and Discussion	34

4.1	Preliminary Studies on CoSO_4 Synthetic Solution	34
4.1.1	Effect of D2EHPA Concentration in the Organic Phase	34
4.1.2	Effect of TBP Additions to the Organic Phase	35
4.1.3	Effect of Cobalt Concentration	36
4.1.4	Effect of Saponifying the Organic Phase.....	36
4.2	Preliminary Study on Synthetic Solutions Containing MnSO_4 , CoSO_4 , CuSO_4 , and NiSO_4 39	
4.3	Study of D2EHPA Extraction Mechanism on Leachate	42
4.3.1	Effect of Initial Concentration of Each Element on E%	42
4.3.2	The Effect of Equilibrium pH on the E%:	46
4.3.3	D2EHPA Loading Percentage as a Function of Initial Concentration of Metal Ions in Leachate.....	48
4.4	Selective Extraction of Mn from the Leachates:	49
4.5	Mn Extraction with 10 and 20 vol% D2EHPA in Kerosene.....	53
4.6	Extraction of Li from Wastewater using HBTA+TOPO	59
5	Future Work:.....	63
6	Conclusion.....	65
7	Bibliography	66
	Appendix A.....	I
	Appendix B.....	III
	Appendix C.....	VIII
	Appendix D.....	XII
	Appendix E.....	XV

List of Figures:

Figure 1.1 – a) cylindrical cell structure, and b) prismatic cell structure [4].....	2
Figure 1.2 - Predicted sales of EVs by 2040 [10].....	3
Figure 1.3 - Flow diagram of LIBs recycling process [1].....	5
Figure 1.4 - The periodic table of endangered elements [16].....	6
Figure 3.1 - Picture on left, sieving set-up and picture on right shows the vacuum filtration set-up.	23
Figure 3.2 - Leaching set-up.	24
Figure 3.3 - Solvent extraction set-up. Top left is shaker, bottom left is separating funnels, top right is the aqueous phase after separation and bottom right is the organic phase after separation.	26
Figure 3.4 - a) the aqueous phases and b) the organic phases after extraction with HBTA+TOPO.	27
Figure 3.5 - Rigaku Supermini200 [35].....	29
Figure 3.6 – a) Prepared concentration vs concentrations obtained by MP-AES, b) regression line equation.....	30
Figure 3.7 - Agilent 4210 instrument [37].....	31
Figure 4.1 - E% as a function of D2EHPA concentration, b) effect of initial Co concentration..	35
Figure 4.2 - Effect of ammonia amount on pH of the organic phase.....	37
Figure 4.3 - Picture on left demonstrate the mixture of the organic and the aqueous phase after shaking, picture on middle shows the mixture after 6h and picture on the right exhibits the organic phase and the aqueous phase after separation.	38
Figure 4.4 - E% of Co as a function of saponification percentage.	39
Figure 4.5 - Extraction efficiency of each element in different synthetic leachate.	41
Figure 4.6 - E% as a function of concentration of each element (g/L).	44
Figure 4.7 - Effect of equilibrium pH on the E%. a) Leachate S/L=95, b) Leachate S/L=120, c) Leachate S/L=95E, d) Leachate S/L=120E.	47
Figure 4.8 - D2EHPA loading percentage vs total number of moles of metal ions in the aqueous phase.	49
Figure 4.9 - Top left picture shows the change in the color of leachate after adjusting the pH to 5.5 by ammonia, the dark blue is the leachate at pH=5.5. Top right demonstrates the precipitates in the	

leachate. Bottom left shows the filter cake after filtration of 2 times diluted leachate. Bottom right shows the small precipitates in the leachates after multiple filtration.	51
Figure 4.10 - Effect of equilibrium pH on E% when D2EHPA concentration was varied, a) Leachate L1, b) Leachate L2, c) Leachate L3.	52
Figure 4.11 - Effect of equilibrium pH and D2EHPA concentration on D2EHPA loading percentage.	54
Figure 4.12 - Effect of saponification percentage on the E% of each element with various D2EHPA concentration.	56
Figure 4.13 - the separation factor of Mn over other elements in different equilibrium pH, a) separation factor Mn over Co and Ni, b) separation factor of Mn over Cu and Al, c) separation factor of Mn over Li.	57
Figure 4.14 - a) E% as a function Li initial concentration, b) Remaining Na in the organic phase as Li initial concentration.	61
Figure 5.1 - The recommended flow diagram for LIBs recycling.	63
Figure 5.2 - Flow diagram for Li recycling from the wastewater.	64

List of Tables

Table 2.1 - Chemical structure of some of the extractant.	13
Table 3.1 - Composition of the organic part.	25
Table 4.1 - Elemental composition of the synthetic leachates, measured by MP-AES.	40
Table 4.2 - Elemental composition of different leachates, measured by MP-AES.	42
Table 4.3 - Equilibrium pH for each set of experiments.	43
Table 4.4 - Equilibrium pH of 3 different set of experiments, each contains 4 different leachate.	46
Table 4.5 - Elemental composition of different leachates, measured by MP-AES.	50
Table 4.6 - Effect of saponification percentage and D2EHPA vol% on equilibrium pH.	53
Table 4.7 - Composition of wastewater determined by MP-AES.	60
Table 4.8 - E% of Li from wastewater without up-concentration.	62

1 Introduction

The application of lithium-ion batteries (LIBs) in portable electronic devices, electric vehicles (EV), and energy storage units has been multiplying in recent years. Due to their excellent performance, such as high energy density, high working voltage, no memory effect, low-discharge rate, lightweight, and long cycle life, they became the most used rechargeable batteries. This increased demand has considerably influenced LIB production, which consequently has led to significantly increased quantities of LIBs waste [1].

LIBs are composed of five main components: anode, cathode, electrolyte, separator, and an outer shell. The cathodes are made of carbon powder, polymer binder like polyvinylidene fluoride (PVDF), and lithium (Li) transition metal oxides such as $\text{LiNi}_{1/3}\text{Co}_{1/3}\text{Mn}_{1/3}\text{O}_2$ (NMC), LiCoO_2 (LCO), LiMn_2O_4 (LMO), and LiFePO_4 (LFP). The anodes are made of graphite, and a polymer binder. Both cathode and anode are coated on aluminum (Al) and copper (Cu) foil as current collectors, respectively [1]. The electrolyte is an organic solvent such as dimethyl carbonate (DMC) and ethylene carbonate (EC) with dissolved Li salts such as LiClO_4 , LiBF_4 , and LiPF_6 [2]. The organic solvent is vital for increasing the mobility of Li ions, and therefore a critical factor in battery performance. The separator is a safety component between the cathode and the anode, preventing direct contact that can cause short-circuiting. As the power is generated from Li diffusion, the separator has to be permeable to Li^+ ions. Common separator materials are polyethylene and polypropylene. The outer shell could be made from stainless steel [1]. Li-ion battery cells are manufactured as cylindrical, stack and prismatic cells [3]. Fig. 1.1 demonstrates two different battery cell structure, cylindrical and prismatic cells.

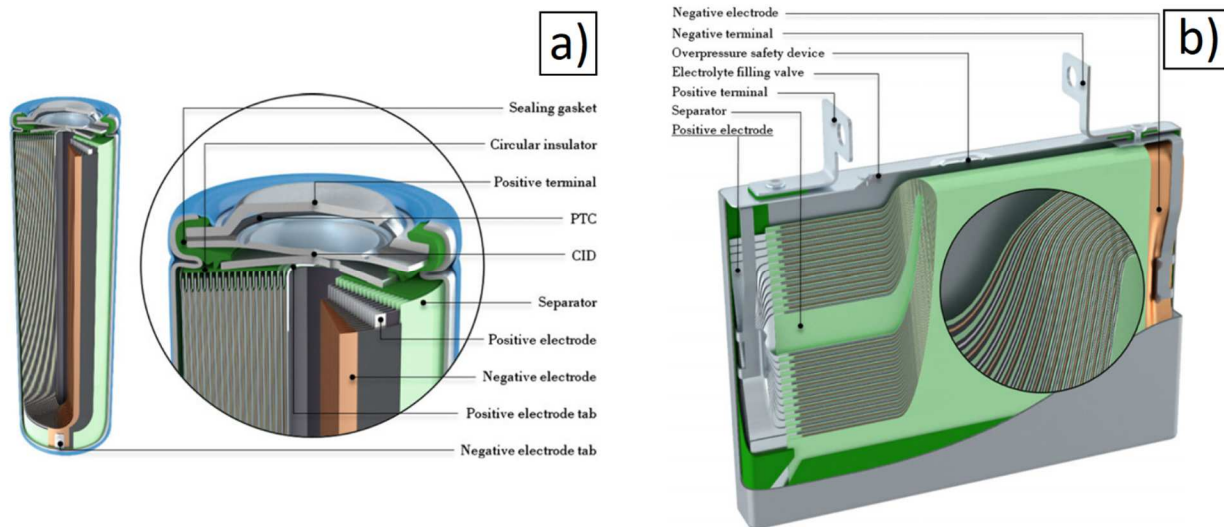


Figure 1.1 – a) cylindrical cell structure, and b) prismatic cell structure [4].

The production of LIBs from raw materials is an energy-intensive process. The materials required to produce the battery cells have high embodied energies. For example, cast Cu has 56–62 MJ/kg, primary nickel (Ni) 159–175 MJ/kg, primary cobalt (Co) 270–300 MJ/kg. Also, mining processes to obtain these elements could be harmful to the environment due to the emission of SO_x [4]. Li content in the earth's crust is about 0.007%, mainly from brines and ores [5]. In order to obtain Li from salt lake brines, large-scale solar ponds are needed, and those consume water in large amounts. Obtaining Li from ores can harm the environment because of the pollution caused by mineral processing [6].

LIBs waste also could be dangerous for human health and the environment. In one life cycle impact assessment, it was revealed that LIBs waste could lower the quality of the environment and human health, mainly in countries with no appropriate infrastructure for waste management. Also, under a particular landfill condition, metal ions such as Co, Cu, and Ni could be leached into the soil with a concentration exceeding regulation in some countries [7].

The other challenge in supplying these raw materials is that the mines are located in a few countries with an unstable government [8]. One of these countries is the Democratic Republic of Congo (DRC), where nearly 75% of people live in poverty. Some of the Co that is mined in Congo comes from small-scale mines, where people and children work in hazardous environments. There are environmental and economic issues regarding supply of scarce elements for LIBs production. In this regard, there are several human rights violation issues [9].

Demand for lithium-ion batteries is increasing remarkably. LIBs are used in various electronic components, from mobiles to electronic vehicles such as electric cars. Global EV sales increased 65% from 2017 to 2018, for 2.1 million vehicles, with sale figures steady through 2019. However, due to the COVID-19 outbreak, the EV sales decreased 25% during the first quarter of 2020. Despite these setbacks, EV demand is again expected to rise, according to Bloomberg New Energy Finance (BNEF). The study finds that EVs will hit 10% of global passenger vehicle sales by 2025, rising to 28% in 2030 and 58% in 2040. Fig. 1.2 demonstrates the predicted EV sale by 2040 [10].

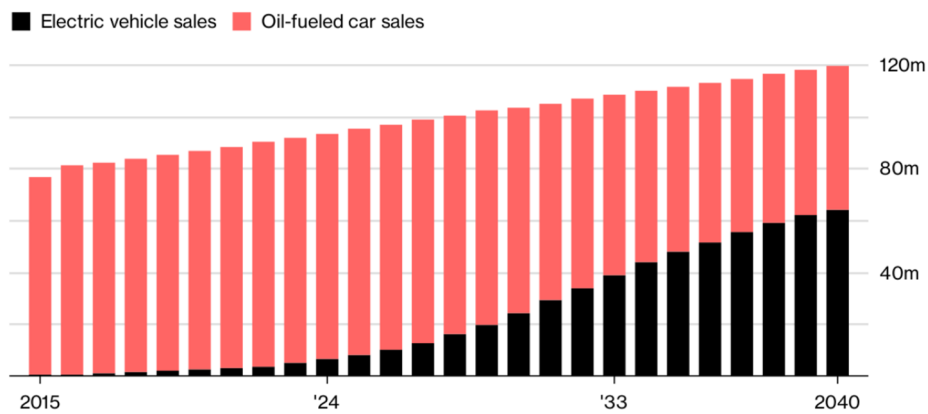


Figure 1.2 - Predicted sales of EVs by 2040 [10].

Increasing demand for LIBs will increase the battery's raw material price. It has been predicted that from 2017 to 2024 LIBs market will grow at the compound and annual growth rate (CAGR) of 12%. For that reason, the production of LIBs will be more challenging by 2050 due to the depletion of primary raw materials such as Co, Ni, and Li [11]. Also, the increasing demand for EVs will make a significant challenge regarding their status after reaching the end-of-life. The large amounts of spent LIBs need to be recycled effectively to minimize the environmental impact and helps the industries to move towards sustainable supply chains.

1.1 An overview on lithium-ion battery recycling

There are two main routes to recycle LIBs, pyrometallurgy or hydrometallurgy. The current pyrometallurgical route is inefficient due to two reasons. First reason is high energy usage, since pyrometallurgical route consists of heat treatment and smelting of LIBs scrap. The second is the loss of valuable metals in slag, especially Li [12]. Also, secondary pollutions, such as hazardous gasses, make the pyrometallurgical process less environmentally friendly. In contrast, the hydrometallurgical route is more efficient. Less energy is used, the recovery rate is much higher due to easier separation, and secondary pollution is lower than the pyrometallurgical route [12]. However, there are some drawbacks for a hydrometallurgical route, for instance high usage of chemicals and complicated recovery routes such as precipitation or solvent extraction. There are some difficulties regarding the separation of metals individually using these techniques since the valuable transition metals (Ni, Co and Mn) have similar properties [13].

Generally, the recycling of LIBs contains three primary steps. The first stage is disassembling and discharging the batteries, the second is leaching using organic or inorganic acid, and the third is recovering targeted metals such as Co, Ni, and Mn from the cathode materials. The discharging step is crucial because if it is not properly performed, it is likely that a short circuit and self-ignition occurs during the pre-treatment steps [1]. Discharging the LIBs is obtainable by submerging the batteries into NaCl solution. In research by Li et al. [14], they studied the effect of NaCl concentrations on discharging efficiency. They found out with 10 wt.% NaCl solution, ideal discharge efficiency is attainable in a reasonable time and cost.

After discharging, the LIBs are dismantled and separated. After dismantling the stainless steel case, the battery core could be removed. The battery core could be divided into the cathode, anode, organic separators, electrolyte, and stainless steel cases. Physical processes can help for better dismantling, such as mechanical separation, thermal treatment like vacuum pyrolysis, mechanochemical processes, and dissolution processes [15]. A shredded cathode or mixture of cathode and anode can be used for the next step.

Leaching is a vital step in the LIBs recycling process. During leaching, cathode active material will convert into metal ions in a solution, and then metals will be recovered from the solution by a series of chemical methods. Different methods can be applied for the leaching step, such as acid

leaching with an organic or inorganic acid, bioleaching, alkaline leaching, and selective leaching and intensified leaching [1]. Leaching will be discussed briefly in Ch. 2.

After leaching, leachate can undergo some chemical processes like precipitation, solvent extraction, and electrochemical processes to recover the valuable metals. In the precipitation methods, reagents that contain ions such as OH^- , $\text{C}_2\text{O}_4^{2-}$, and CO_3^{2-} will be added to the leachate. Metal ions present in the leachate will be reacted to these reagents and form a precipitate. In the electrochemical processes, metal ions will be separated due to their different electrochemical potential [1]. Solvent Extraction will be discussed thoroughly in Ch. 2. Fig. 1.3 presents a flow diagram for LIBs recycling.

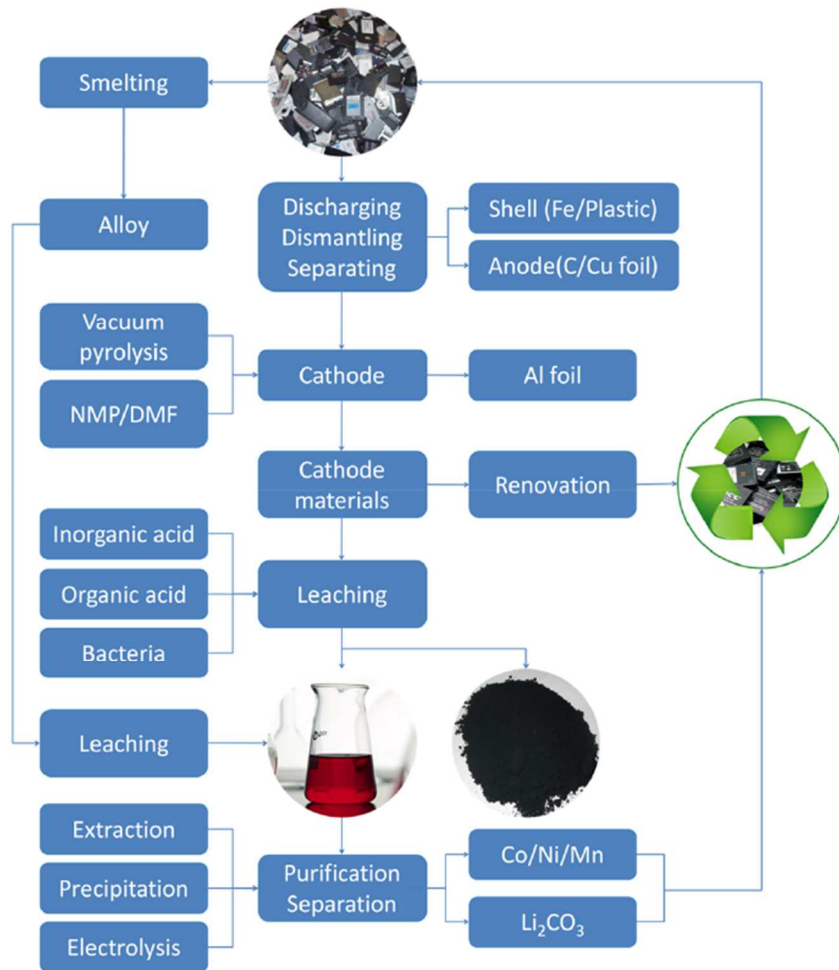


Figure 1.3 - Flow diagram of LIBs recycling process [1].

1.2 Goals and Motivation

Sustainable recycling of spent LIBs exhibits a promising research field for both environmental protection and valuable materials re-utilization. Due to the increasing demand of LIBs, a large number of Ni, Mn, Co, and Li resources are needed for the future production of LIBs. Fig. 1.4 demonstrates that all of the mentioned elements are considered as endangered elements and they face critical supply risks [16]. Recycling of these metals from spent LIBs can help solve the environmental issues and relieve the shortage of raw materials. New EU regulation also requires a 35% recovery rate for lithium from LIBs by 2025 and a 70% recovery rate by 2030. Moreover, material recovery rates for other elements should be 90% in 2025 and 95% in 2030 [17].

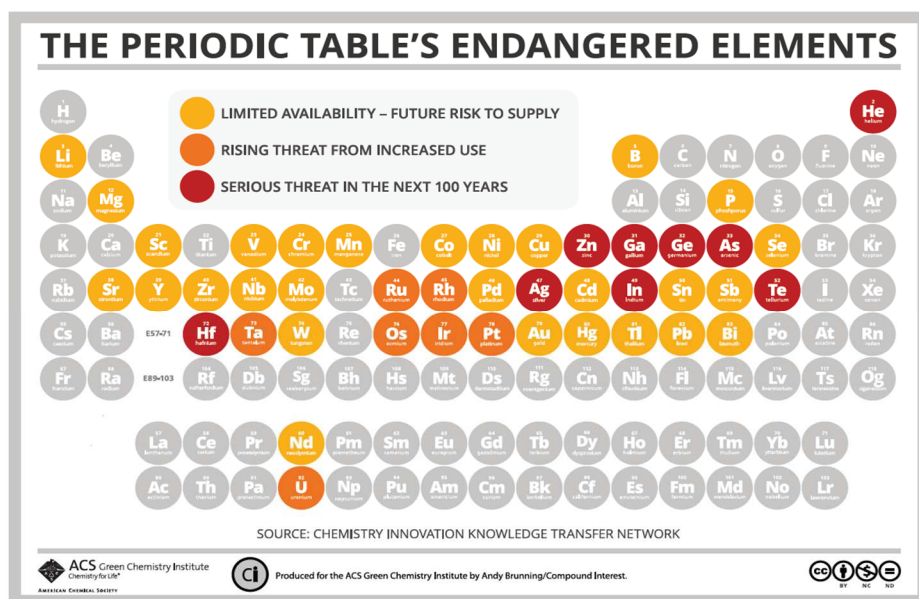


Figure 1.4 - The periodic table of endangered elements [16].

This thesis aims to investigate the extraction behavior of transition metals such as Co and Mn from an acidic environment (leachates of spent LIBs, sulfate-based). Furthermore, the extraction mechanism of Li from wastewater of spent LIBs crushing will be studied.

- Bis (2-Ethylhexyl) phosphate (D2EHPA) will be utilized to study the extraction behavior of divalent ions from leachates of spent LIBs. Effect of equilibrium pH, extractant

concentration, and initial concentration of metal ions on extraction efficiency will be investigated.

- 4,4,4-trifluoro-1-phenyl-1,3-butanedione (HBTA) will be used to extract Li from the wastewater. The extraction mechanism of HBTA and the effect of initial Li concentration on extraction efficiency will be studied.

1.3 Thesis Outline

The thesis consists of 6 chapters, starting with the importance of LIBs recycling and the project's motivation. Chapter 2 is an overview of the theory behind leaching and solvent extraction. Also, publications relevant to this thesis have been discussed in chapter 2. Chapter 3 describes the experimental procedure and the methodology. Chapter 4 contains results from the experiments, followed by a discussion of the results. Also, future research possibilities and ideas were mentioned in chapter 5. The conclusion of the conducted work is given in chapter 6. Appendix, downloadable files, and list of publications are provided.

2 Theory and Literature Review:

In this chapter, a brief introduction to leaching will be discussed. Furthermore, solvent extraction will be thoroughly reviewed since this thesis aims to utilize solvent extraction for metal recovery from spent LIBs. At last, some of the previous studies related to this thesis will be reviewed.

2.1 Leaching:

Leaching is a solid-liquid mass transfer process and a crucial step for recovering valuable metals from spent LIBs in the hydrometallurgical process. Leaching aims to convert the metals in the cathode active materials obtained from the previous pretreatment process (such as dismantling and separation) to ions in a solution. These ions can therefore be extracted selectively from the solution with a series of chemical procedures such as solvent extraction, precipitation, etc. Leaching can be carried out at ambient conditions or elevated temperatures and under pressure. The process conditions will depend on chemical reactions taking place. The leaching of battery materials is usually carried out using inorganic acid, organic acid, or alkali leaching reagents. Sometimes, some assistant measures, such as ultrasonic waves and mechanical chemistry, are employed to enhance the leaching process [1].

Many parameters can affect the leaching process, such as acid concentration, surface area, particle size, the solid matrix's pore size, homogeneity of solids, temperature, agitation, mineralogy, intermediate products, and crystal structures. When H_2SO_4 concentration increased, the leaching efficiency increased [18]. The solid to liquid ratio is defined as the fraction of the total solid material's dry mass to the total liquid (leaching reagent) volume. When it comes to solid to liquid ratio, leaching efficiencies were increased with the decrease in solid to liquid ratio. Less solid to liquid ration means higher surface area available for reaction to happen. Leaching is affected by temperature. In general, a higher temperature will lead to faster leaching kinetics; however, the exact relation between temperature and leaching rate is dependent on the type of the leaching reaction (diffusion-controlled or reaction-controlled leaching). Agitation also affects the leaching kinetics by reducing the diffusion layer's thickness. If the leaching is reaction-controlled, the rate is not affected significantly since the chemical reaction is much slower than the diffusion through

the diffusion layer. In diffusion-controlled leaching, the leaching rate will increase due to decreased diffusion layer thickness [19].

Several inorganic acids such as H_2SO_4 , HCl , and HNO_3 are commonly used leaching agents for cathode active materials leaching. H_2SO_4 and HNO_3 was usually used in the presence of a reducing agent such as H_2O_2 , NaHSO_4 or glucose. The reducing agent can convert the metals in the cathode active materials to their divalent states, for example, Co^{+3} to Co^{+2} , Mn^{+4} to Mn^{+2} , which are more soluble in acid solutions [1].

2.2 Solvent Extraction Fundamentals:

Solvent extraction is widely used in hydrometallurgical processes. In solvent extraction, metal ions will be separated due to their different relative affinity to the compounds in the organic phase. The targeted metal ions in the aqueous phase will be transferred to the organic phase, and then they the two phase be separated due to the difference in their density [20].

Solvent extraction contains three main steps, extraction, scrubbing, and stripping. In the extraction part, leachate that contains the metal ions will be contacted with an organic solvent that is immiscible with the leachate. Transfer of metal ions depends on the extraction condition and the nature of the organic part. If everything is set correctly, a complete transfer of targeted metal ions is probable. At the end of extraction, the organic phase will be separated from the aqueous part due to its density. Then, the organic part is brought into contact with a scrubbing solution. Scrubbing solution is an aqueous solution, and it helps eliminate the impurities that are co-extracted with the targeted metal ion. Scrubbing can be done by an acid solution or alkali salt. Scrubbing can certify the production of high purity metal. Stripping is the final part, and it is a reverse action of the extraction part. The scrubbed solution, which is the organic phase without the impurities, will be contacted with an aqueous solution called strip solution, and the metal ion in the organic part will be transferred to the aqueous phase. Stripping solution is a solution acid or alkali or a dilute solution of the targeted metal ion. Regeneration of solvent is essential since the solvent could be damaged during the process. Regeneration will be done by contacting the solvent with the proper alkali or acid solution [20].

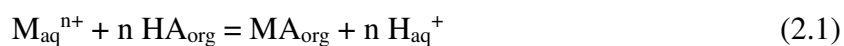
For lab scale procedure, single-stage extraction is preferred. Therefore, a high distribution coefficient, high selectivity, and high separation factor are needed, these factors will be explained

thoroughly in sub-chapter 2.2. Since extraction is done in a multi-stage and counter-current manner on an industrial scale, a low distribution and separation factor is acceptable. The extraction and stripping rate is not essential for lab-scale extraction, but it has an essential role in industrial scale due to economics [20].

2.2.1 Extractant Mechanisms:

Most of the metal salts can quickly dissolve into the water. After the dissolution of metal salts, water molecules will be bonded to the metal ions, and the coordination number of the metal regulates the number of these water molecules. Organic solvents are non-polar, and metal ions cannot transfer to the organic part. To transfer the metal ion to the organic part, the water bonds should be broken, and the metal ion should be neutralized. These are attained by forming a neutral complex soluble in the organic phase or a direct reaction between metal ions and a suitable organic compound to form a neutral complex. Based on the extraction mechanism, organic extractants are of three types: Cationic (acidic), anionic (primary), and Solvating (Neutral) [20].

Cationic extractant operates through the cation exchange between the organic and aqueous phases. A neutral complex will be formed by replacing one proton (H^+) in the extractant for every positive charge on the metal. The cation exchange processes could be done either by chelate formation or by acid extraction. In the chelate formation, the transfer of metal ions happens due to the formation of electrically neutral metal chelate with the chelating agent's aid. The chelating agent should satisfy the valance and coordination number of the metal ions. Organic solvents that contain both acidic and basic groups will be combined with metal ions, and chelate salt will be formed. The following reaction presents chelate extraction:

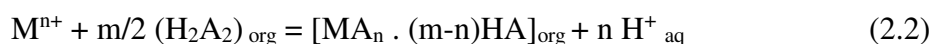


Where HA_{org} is the chelating agent and M_{aq}^{n+} is the metal ion [20].

For example, benzoyltrifluoroacetone (HBTA) is a β -diketones and acts as an acidic chelating extractant. The β -diketone is a diketones in which a single carbon atom separates the two ketone groups. Diketones are organic compounds containing two carbonyls ($C=O$) bonds, and a ketone is a functional group with the structure $R_2C=O$, where R can be a variety of carbon-containing substituents.

The reaction shows that exchange results in a higher concentration of hydrogen ions in the aqueous phase. Therefore, extraction with chelating extractant needs a precise control of acid concentration. Higher H^+ concentration can cause the reaction to go backward direction and hinder the extraction [20].

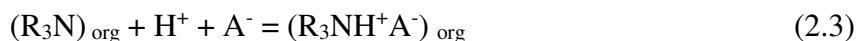
Acid Extraction mechanisms are more complicated than chelating extractants because they are affected by solvent properties. Organophosphorus and carboxylic acids form polymer dimers in the organic phase that affect their extractive properties. Alkyl carboxylic, phosphoric acids, and sulfonic acids are acid extractant. The following reaction could represent the extraction:



H_2A_2 represents the dimeric form of the extractant and “m” is the total number of extractant molecules in extracted species. From the reaction, it is clear that extraction will be improved as the metal becomes more basic. So careful control of the pH is needed. If the metal ions have the same charge, their extractability varies reciprocally with the ionic radius [20].

Ionquest 801 (2-ethylhexyl phosphonic acid mono-2-ethylhexyl ester), Cyanex 272 (di-2,4,4-trimethylpentyl-phosphinic acid) and D2EHPA (di-(2-ethylhexyl) phosphoric acid) are the example of acidic extractant. The literature reported that the separation of Co from Ni in sulfuric media is possible using acidic extractant [21]. The separation ability increases in phosphinic >phosphonic>phosphoric due to the increasing stability of Co tetrahedral in the organic phase [21]. Organophosphorus extractant such as D2EHPA is very effective for separating Mn and Cu in sulfuric acid media [22].

The anionic extractant is an extractant that acts as an anion exchanger. To use these types of extractant, metal ions should form an anionic complex in the aqueous phase. A limited number of metals can form an anionic complex under certain circumstances; therefore, anionic extractant selectivity is very high. Long-chain alkylamines are widely used in anionic extraction. The extraction reaction is indicated below:

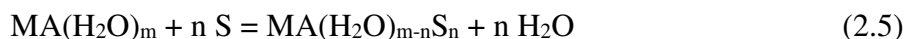


Where A^- is metal anionic complex in the aqueous phase. From the reaction, it is evident that extraction is increasing in acidic solution due to high concentration of hydrogen ion and it is hindered in basic solutions [20].



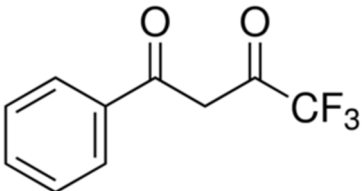
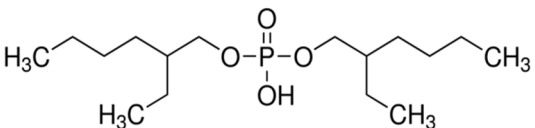
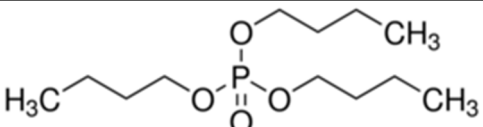
From the reaction it is clear that a metal ion can be extracted by alkylamines if it forms an anionic complex in the water [20].

Neutral (solvating) extractant will facilitate the extraction by replacing themselves with water molecules that are bonded to the metal ion and formed a neutral complex by ion association. Some organic reagents such as alcohols, ethers, ketones, and alkyl phosphate with an O atom as an electron donor can act as a solvating extractant. Tributylphosphate (TBP) is one of the most well known solvating extractant. The reaction for this type of extractant can be expressed as below, where S is the solvent and $MA(H_2O)_m$ is metal complex in the aqueous phase [20].



Other than these three main types of extractant, sometimes two extractants from different groups will be mixed to obtain a synergetic effect. The extractant that shows typically low to no extraction of a targeted metal ion will be added to the extractant known for its ability to extract targeted metal ions. For example, D2EHPA extracts uranium from sulfuric acid media, but TBP cannot extract it. If TBP is added to D2EHPA, the extraction by D2EHPA will significantly increase. Therefore, TBP acts as a synergetic component [20]. Another example is a β -diketone system (HBTA) and a neutral extractant for Li extraction. Trioctylphosphine oxide (TOPO) is a neutral extractant that can not extract Li from the aqueous feed. However, when TOPO is added to HBTA, which can extract Li, the extraction efficiencies for Li will increase remarkably since the chemical complex of Li.HBTA.TOPO is more stable in the organic phase [6]. Table 2.1 demonstrates the different type of extractants.

Table 2.1 - Chemical structure of some of the extractant.

Name of Extractant	Type	Chemical Structure
HBTA	Cationic Extractant, Chelating	 <p style="text-align: right;">[23]</p>
Cyanex 272	Cationic Extractant, Acidic	$\text{CH}_3(\text{CH}_2)_4\text{CH}_2-\overset{\text{CH}_2(\text{CH}_2)_4\text{CH}_3}{\underset{\text{CH}_2(\text{CH}_2)_4\text{CH}_3}{\overset{+}{\text{P}}}}-\text{CH}_2(\text{CH}_2)_{12}\text{CH}_3$ <p style="text-align: right;">[24]</p>
D2EHPA	Cationic Extractant, Acidic	 <p style="text-align: right;">[25]</p>
Aliquat-336	Anionic Extractant, Quaternary amine	$\text{CH}_3(\text{CH}_2)_6\text{CH}_2-\overset{\text{CH}_3}{\underset{\text{CH}_2(\text{CH}_2)_6\text{CH}_3}{\overset{+}{\text{N}}}}-\text{CH}_2(\text{CH}_2)_6\text{CH}_3 \quad \text{Cl}^-$ <p style="text-align: right;">[26]</p>
TOPO	Neutral Extractant	$\text{CH}_3(\text{CH}_2)_6\text{CH}_2-\overset{\text{O}}{\underset{\text{CH}_2(\text{CH}_2)_6\text{CH}_3}{\overset{=}{\text{P}}}}-\text{CH}_2(\text{CH}_2)_6\text{CH}_3$ <p style="text-align: right;">[27]</p>
TBP	Neutral Extractant	 <p style="text-align: right;">[28]</p>

2.2.2 Additives in Solvent System:

The Organic part contains some additives such as diluents and modifiers in addition to the extractant. The diluent is added to modify physical properties such as viscosity and density for better mixing. Diluents are aromatic or aliphatic hydrocarbons, and they do not have an extraction capacity, but they can significantly affect the processes. The most common diluent is kerosene. Modifiers are often added to the solvent system to inhibit the formation of the third phase and facilitate the metal complex. They are long-chain alkyl alcohols or a neutral extractant such as Tributyl phosphate (TBP). Modifiers also influence the extraction processes, so they need to be chosen very carefully [20].

2.2.3 Thermodynamics of Solvent Extraction:

The extraction equilibria depends on the extractant type. For a cationic extractant, the reaction can be expressed by reaction (2.6); the focus on this chapter would be on cationic extractant since both D2EHPA and HBTA are cationic extractants.



The thermodynamic equilibrium constant K'_{ex} can be described by the following equation:

$$K'_{ex} = \frac{[H^+]^n \cdot [MA_n \cdot (m-n)HA]_{org}}{[H_2A_2]_{org}^{\frac{m}{2}} \cdot [M^{n+}]_{aq}} \cdot F \quad (2.1)$$

Where the F is ratio of molar activity coefficients. Then the extraction constant K_{ex} is:

$$K_{ex} = \frac{K'_{ex}}{F} = \frac{[H^+]^n \cdot [MA_n \cdot (m-n)HA]_{org}}{[H_2A_2]_{org}^{\frac{m}{2}} \cdot [M^{n+}]_{aq}} \quad (2.2)$$

Distribution coefficient or ratio can be defined as the total amount of solute in organic phase to that in the aqueous phase. The higher the distribution coefficient, the better.

$$D = \frac{[MA_n \cdot (m-n)HA]_{org}}{[M^{n+}]_{aq}} \quad (2.3)$$

The expression for K_{ex} can be written as a form of D:

$$K_{ex} = \frac{[H^+]^n \cdot D}{[H_2A_2]_{org}^{\frac{m}{2}}} \quad (2.4)$$

$$\log D = \log K_{ex} + n pH + \frac{m}{2} \log [H_2A_2] \quad (2.5)$$

Equation (2.5) shows that higher K_D can be obtained by higher pH and higher concentration of the extractant. Equation (2.6) can be used for calculating the percent extraction.

$$\text{Percent extraction} = \frac{w - w_1}{w_1} \cdot 100 = \left[1 - \frac{w_1}{w} \right] \cdot 100 = \frac{100 D}{D + \frac{V_A}{V_O}} \quad (2.6)$$

Where w is the original weight of metal ion in aqueous phase before extraction, w_1 is the weight of metal ion left in the aqueous phase after extraction, V_A is the volume of the aqueous phase and V_O is the volume of the organic phase. Percent extraction increase when V_A/V_O decreases. Therefore, higher O/A ratio is desired [20].

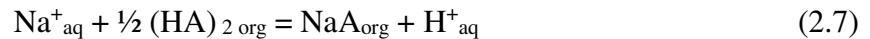
When it comes to separating two chemically similar metal present in aqueous phase, separation factor plays an important role. Separation factor between A^{n+} and B^{m+} for cationic extractant can be defined as:

$$\beta = \frac{(D)_{A^{n+}}}{(D)_{B^{m+}}} \quad (2.7)$$

Separation factor should be higher than 1 to successfully separate two metals [20].

2.2.4 Saponification of Organic Phase

Acidic extractants such as D2EHPA, Cyanex 272, and PC-88A can be neutralized using sodium hydroxide or ammonia. Equation (2.7) describes the neutralization reaction using sodium hydroxide.



The extractant's neutral form exists as a monomer, whereas the acidic form is a dimer. Both forms take part in the extraction. The mechanism by which a divalent metal ion is extracted from an aqueous phase using the partially neutralized cation exchange extractant follows the reaction as given below [29].



The equilibrium constant, K , for the above reaction can be described as below

$$K_{ex} = \frac{[H^+]. [MA_3.3HA]_{org}}{[(HA)_2]^2. [M^{2+}]_{aq}. [A^-]_{org}} \quad (2.8)$$

Alternatively, it can be described as below by using $D = [MA_3.3HA]_{org} / [M_{aq}^{2+}]$.

$$K_{ex} = \frac{[H^+]. D}{[(HA)_2]^2. [A^-]_{org}} \quad (2.9)$$

Taking logarithm and arranging the Equation (2.9) will give the Equation (2.10):

$$\log D = \log K + pH + \log [A^-]_{org} + 2 \log [HA_2]_{org} \quad (2.10)$$

Analyzing the experimental value of distribution ratio as a function of equilibrium pH and extractant concentration at a constant value of other parameters allows estimation of the number of extractant molecules associated with the extracted metal complex [29].

2.3 Reviews and Previous Studies

Solvent extraction can be used to separate and recover metal ions from the leachate of spent lithium-ion batteries. For lithium-ion batteries, various extractants such as PC-88A, D2EHPA, and Cyanex272 are used for metal recovery [15].

Swain et al. [30] developed a hydrometallurgical route for the recycling of lithium-ion batteries wastes. They first leached the batteries using sulfuric acid and hydrogen peroxide to obtain a leachate containing cobalt sulfates. After they optimized the leaching step, they performed a solvent extraction on the leachate containing 44.72 g/L Co and 5.43 g/L Li at a pH of 5.00. Cyanex 272 was used as an extractant, and it saponified to 65% by NaOH. Kerosene and tributyl phosphate (TBP) were used as diluents and modifiers, respectively. The pH of leachate was adjusted by sulfuric acid or sodium hydroxide. All the experiments were carried out at room temperature (25 °C) and the time for reaching the equilibrium was 10 minutes. They studied the effect of pH, Cyanex concentration, and organic to aqueous ratio (O/A).

The pH was studied with O/A=1 and Cyanex concentration of 1M. They found out that the maximum extraction for cobalt was 51.23% at an equilibrium pH of 5.35 (initial feed pH of 5). In this equilibrium pH, the separation factor was highest, and only 8% of lithium was co-extracted. The effect of Cyanex concentration was studied at an initial pH of 5 and O/A=1 and, Cyanex concentration was varied from 0.5 to 2M. They discovered that by increasing the concentration,

the extraction of both cobalt and lithium were increased. Although higher concentration led to higher extraction, a higher concentration is inefficient due to viscosity, phase disengagement, and scrubbing difficulties. Furthermore, the concentration of 1.5M was chosen.

The O/A ratio effect was studied at an initial pH of 5 and the Cyanex concentration of 1.5M. Recovery of both lithium and cobalt increased when the O/A ratio increased. At an O/A ratio of 2, Co and Li's recovery was 99% and 40%, respectively. They observed that by increasing the O/A ratio, Co content in the organic phase would be decreased; however, it will be increased for Li. Since Co content decreased and Li content increased in the organic phase, the cobalt purity decreased in the organic phase with an increase in O/A ratio. Hence, for higher scrubbing efficiency, the O/A ratio of 1.6 was chosen. At this O/A ratio, the extraction efficiency of cobalt was 85%.

In a paper by Wang et al. [31], they obtain leach liquors by leaching the cathodes of spent lithium-ion batteries in sulfuric acid. Then they have done a two-step extraction using D2EHPA and PC88A as an extractant and sulfonated kerosene as a diluent. The first extraction was done using D2EHPA to extract Cu and Mn. Saponification rate was 20%, D2EHPA concentration was 30 vol%, O/A=1, extraction time of 10 minutes, and the pH is equal to 2.7. Then PC88A was used to separate Co from Ni under the saponification rate of 30%, PC88A concentration of 30 vol%, O/A=1, extraction time of 10 minutes, and pH equal to 2.6.

Hu et al. [32] studied the solvent extraction process on a solution containing 16.3 g/l Ni, 0.7 g/l Co, 0.6 g/l Ca, and 1.6 g/l Mg. D2EHPA and Cyanex 272 were used as an extractant. Both extractants were saponified with NaOH and diluted in Kerosene. The extraction process was carried out in an incubator shaker at room temperature for 10 minutes, and the organic to aqueous ratio was one. They concentrated the solution to obtain 89.2 g/l Ni, 4.3 g/l Co, 0.6 g/l Ca, and 7.7 g/l Mg and studied the Ca removal using D2EHPA. The effects of the extraction parameters such as equilibrium pH and D2EHPA concentration were assessed. The extraction order of the metal ions follows $Ca > Mg > Co > Ni$. At equilibrium pH = 1.6, the extraction efficiency of Ca with 20 vol% Na-D2EHPA was found to be 74%, and this was seen to increase until a maximum of 93% at equilibrium pH = 3. Over this same equilibrium pH range, Mg's respective extraction efficiencies changed from 7% to 23% and Co from 1% to 13%, while the Ni extraction remained insignificant, less than 2%. At equilibrium pH higher than 3, extraction of Ni, Co, and Mg

increased, while Ca's extraction decreased slightly due to Ni's crowding-out effect. After a single contact with 10 vol% Na-D2EHPA at equilibrium pH = 2.5, more than 89% of Ca could be extracted, while the extractions of Mg (10.5%), Co (7.2%) and Ni (0.6%) are much lower. With the increase of equilibrium pH to 3, approximately 91% Ca, 16% Mg, 8% Co and 1% Ni were extracted. Consequently, 10 vol% Na-D2EHPA and equilibrium pH = 2.5 were chosen as the optimum conditions. Then Ca free solution was used for Co recovery using Cyanex 272.

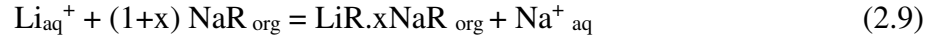
The new solution contained approximately 67.5 g/l Ni, 3.8 g/l Co and 6.3 g/l Mg, and the pH was set to around 5.5 by using 10 M NaOH before extraction using saponified Cyanex. The effects of the extraction parameters such as equilibrium pH and Na-Cyanex concentration were studied. The extraction efficiencies of Co and Mg gradually increase with the increase of equilibrium pH. When the pH value is less than 5.2, Co and Mg's extraction efficiencies are 95% and 44%, respectively, while Ni's extraction is less than 2%. When pH increased to 5.6, the Co and Mg extraction efficiencies reached 97% and 51%, respectively. When the Na-Cyanex 272 concentration increased from 10 vol% to 30 vol% at pH of 5.5, an increase in the extraction of all metal ions was observed, mostly Mg. The extraction efficiency of Ni is relatively high at 5% with 30 vol% Na-Cyanex 272. Therefore, 20 vol% Na-Cyanex 272 was selected to be the optimum concentration required to extract Co and Mg selectively.

Song et al. [33] investigated lithium's extraction process from Li_3PO_4 leaching liquor using saponified D2EHPA. The organic phase consisted of 40 vol% D2EHPA, 10 vol% modifiers (tributyl phosphate (TBP), trialkyl phosphine oxide (TRPO), or 2-octanol), and diluent sulfonated kerosene. D2EHPA was previously saponified by using 10 M NaOH, and the saponification ratio was 70%. The aqueous phase was obtained by dissolving Li_3PO_4 in HCL, it contained 10 g/L Li, and pH was 2.8. The extraction processes were carried out in a water bath at 35 C for 15 minutes, and the O/A ratio was equal to 5. The effect of modifiers, TBP concentration, and the extraction mechanism was studied.

The addition of modifiers, TBP, or TRPO had little effect on Li extraction. D2EHPA exists as a dimer form in non-polar solvent and addition of modifier such as TBP help with depolymerizing the dimers into monomers, therefore, more molecules available for extraction. Since D2EHPA was saponified before and the dimers dissociated into monomers, the addition of TBP had a little effect. Although modifiers' addition had an insignificant impact on extraction, adding TBP promoted Li's

stripping process. Therefore, TBP was chosen as a modifier for the next steps. As previously mentioned, TBP only helps with the stripping process. When the TBP concentration reached 10 vol%, the stripping rate increased and went to 72%. However, increasing the TBP concentration to 15% did not significantly affect the stripping rate. Therefore 10 vol% TBP was chosen.

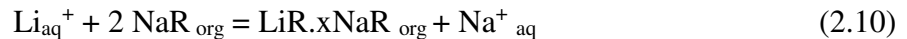
Saponified D2EHPA primarily extracts lithium by replacing Na in the organic phase one by one. The extraction reaction can be written down as bellow:



Then, equilibrium constant K_{ex} , can be written the same way as Equation (2.4). Then Equation (2.11) can be obtained by taking log of the K_{ex} equation.

$$\log ([\text{Na}^{+}] \cdot D_{\text{Li}}) = \log K_{\text{ex}} + (1 + x) \log([\text{NaR}]_{\text{org}}) \quad (2.11)$$

The experiments were done by varying D2EHPA concentration from 30 vol% to 50 vol% in kerosene, and then after separation, Li^{+} and Na^{+} concentration in the aqueous phase can be measured. Therefore, D_{Li} can be determined. One can estimate the concentration of $[\text{NaR}]_{\text{org}}$ in the equilibrium by subtracting the concentration of extracted Li from the initial NaR concentration. Taking $\log ([\text{Na}^{+}] \cdot D_{\text{Li}})$ as the Y-axis, $\log ([\text{NaR}]_{\text{org}})$ as the X-axis, the experimental data can be fitted and plotted. The slope of the fitted line is 1.87, which is close to 2. That means the saponified D2EHPA extracts lithium by combining two D2EHPA molecules with Li^{+} . Therefore, the Reaction (2.9) can be written as below:



Zhang et al. [6] investigated a novel lithium recovery process from effluent of spent LIBs recycling by solvent extraction. The β -diketone extraction system used in the experiment was composed of benzoyltrifluoroacetone (HBTA), trioctylphosphine oxide (TOPO), and kerosene. The effective parameters such as solution pH value, saponification degree, initial lithium concentration, and phase ratio were assessed by experiments.

To study the effect of the aqueous phase pH value on lithium extraction, the experiments were done using 0.4 M HBTA + 0.4 M TOPO in kerosene and the organic and the aqueous phase were mixed using a shaker for 6 minutes at room temperature with O/A=1. The extractants HBTA and

TOPO showed a strong synergist effect, and the effect reached the peak when the concentration of HBTA and TOPO was at the same level.

The effect of aqueous phase pH was studied by change the pH of the feed solution from 1 to 13. It can be concluded that with an increase in the pH of the feed solution, lithium extraction was enhanced. Lithium extraction efficiency reached 80% when the pH was 13. Saponification of the organic phase also affects lithium extraction. The experimental data revealed that lithium extraction is increased with the increase of saponification degree. The increase in lithium extraction slowed down when the saponification degree exceeded 70%. Due to the lower utilization of sodium hydroxide, lithium in the organic phase was almost unchanged with sodium. Therefore, 70% saponification of the organic phase would be proper. The extraction efficiency for lithium by saponified organic is relatively low when the feed solution pH is less than 5, while it increased for a pH value higher than 6. It could be concluded that the replacement between lithium in the aqueous phase and sodium in the organic phase requires that the equilibrium pH of the aqueous phase should be in neutral or alkaline conditions.

The effect of extraction time was also investigated. The lithium extraction reached equilibrium within 2 min, with about 80% extraction efficiency. An increase in contacting time had almost no effect on lithium extraction. Due to the high sodium concentration in the aqueous phase, more sodium will probably transfer to the organic if the extraction duration is too long. To ensure lithium extraction and avoid too much sodium entering the organic phase, 2 min is enough.

They also studied the effect of lithium concentration by changing the initial lithium concentration from 0.029 mol/L to 0.720 mol/L at a constant sodium concentration (1.370 mol/L). The extractant was 70% saponified, and the phase was ratio O/A=1. The extractants' lithium capacity increased from 0.027 mol/L to 0.261 mol/L with the increase of lithium concentration from 0.029 mol/L to 0.720 mol/L. When extractants are mixed with high lithium concentration, they become saturated with lithium; therefore, they can not extract other ions. The effect of the O/A ratio was also investigated. When the O/A increased, lithium extraction decreased significantly. At O/A=1:15, lithium extraction reached less than 20%. With O/A=2:1, lithium extraction efficiency was high, but the separation time was longer. From an economic and operation point of view, it is better to keep the O/A ratio 1.

Based on all the literature presented above, extractant concentration, equilibrium pH, the aqueous feed initial concentration, and the O/A ratio are essential parameters that affect the extraction efficiencies of the systems. Therefore, these parameters will be studied for the extraction systems on this project.

3 Experimental Procedure and Methodology:

3.1 Materials:

In this sub-chapter, chemical reagents and experimental set-up are introduced.

3.1.1 Chemical Reagents:

- **Starting Materials:** Wastewater was obtained by wet-crushing the batteries. The procedure of the wet-crushing will be explained later in this chapter. Leachates were obtained from performing leaching on the crushed battery powders. Leaching reagents used in this study were sulphuric acid (H_2SO_4 , 95%, TECHNICAL, VWR) and hydrogen peroxide (H_2O_2 , 35 wt.%, ACS reagent, Sigma-Aldrich). The leaching was only performed to obtain the starting material (leachates) for the solvent extraction experiments.
- **Solvent Extraction Experiments:** Asol D80 (99.9%, Univar) and Kerosene (100%, reagent grade, Sigma-Aldrich) were used as diluents. 4,4,4-Trifluoro-1-phenyl-1,3-butanedione (HBTA, 99%, Sigma-Aldrich), trioctylphosphine oxide (TOPO, 99%, ReagentPlus®, Sigma-Aldrich) and bis(2-Ethylhexyl) phosphate (D2EHPA, 97%, Sigma-Aldrich) were used as extractants. Tributyl phosphate (TBP, 99%, Sigma-Aldrich) was used as a modifier. Sodium hydroxide (NaOH, Merck Millipore) and Ammonia (NH_4OH , 25 wt.%, EMSURE®, Merck) were used as saponification reagents.
- **Synthetic Solutions:** Manganese (II) sulphate monohydrate ($\text{MnSO}_4 \cdot \text{H}_2\text{O}$, >99%, ACS reagent, Sigma-Aldrich), cobalt (II) sulphate heptahydrate ($\text{CoSO}_4 \cdot 7\text{H}_2\text{O}$, >99%, ReagentPlus®, Sigma-Aldrich), nickel (II) sulphate hex hydrate ($\text{NiSO}_4 \cdot 6\text{H}_2\text{O}$, >98%, ACS reagent, Sigma-Aldrich) and copper (II) sulphate (CuSO_4 , >99%, ReagentPlus®, Sigma-Aldrich) were used to prepare the synthetic leachates. All the synthetic solutions were prepared using deionized water (DI).

3.1.2 Experimental Set-Up:

- **Wet Crushing of Spent LIBs:** Two different types of crushing were done, crushing without the electrolyte and crushing with the electrolyte. In crushing without the electrolyte, the discharged spent LIBs were opened by a rotary saw, and then the steel case was removed. After removing the steel case, the battery core was unfolded, the electrolyte was removed, and the plastic film was separated manually. The anode and cathode foils

were dried overnight and then wet crushed together in a blender, wet crushing means that DI water will be used as a medium. In crushing with the electrolyte, after opening the battery and removing the steel case, the whole battery core with the electrolyte was wet crushed with the same blender. Once the anode and cathode were thoroughly crushed, a mixture of all cell internal materials was achieved. Then the mixture was filtered through 3 metal sieves. The sieves were sized at 11.20, 1.4, and 0.85mm. The sieved solution was then filtered with a vacuum filter to obtain the wastewater. Filtration was done two times to ensure that the wastewater is free of any particles and entirely transparent. The filter cakes, mainly containing the solid smaller than 0.85 mm, the so-called black mass, were used in the subsequent leaching step. Fig. 3.1 demonstrates the metal sieves and the vacuum filtration set-up. Black mass is a mixture of the material used to coat the anode (Cu) and cathode (Al) foils, i.e. the active materials (graphite and metal oxides), binder and additives such as active carbon.



Figure 3.1 - Picture on left, sieving set-up and picture on right shows the vacuum filtration set-up.

- **Leaching Procedure:** The black mass from the previous step was used as a starting material in this step. Two different types of powders were obtained from crushing; with and without electrolytes. Leaching experiments utilizing the electrolyte-containing powder are denoted “E”. The leaching was done at two different solid to liquid ratios (S/L), 95 and 120, for two powder types. The solid was battery powder and the liquid was the leaching reagent. The calculated volume of leaching reagent (2 M H₂SO₄ + 3.75 wt.% H₂O₂) was measured with a measuring cylinder and added to a 250 ml reactor, then 7.5g of powder was weighed and added into the reactor. The reactor was attached to a thermal bath, the temperature was set to 65°C, and the stirring speed was set to 750 rpm. After 1 h, the solution was filtered to obtain the leachates. Fig. 3.2 demonstrates the leaching set-up.

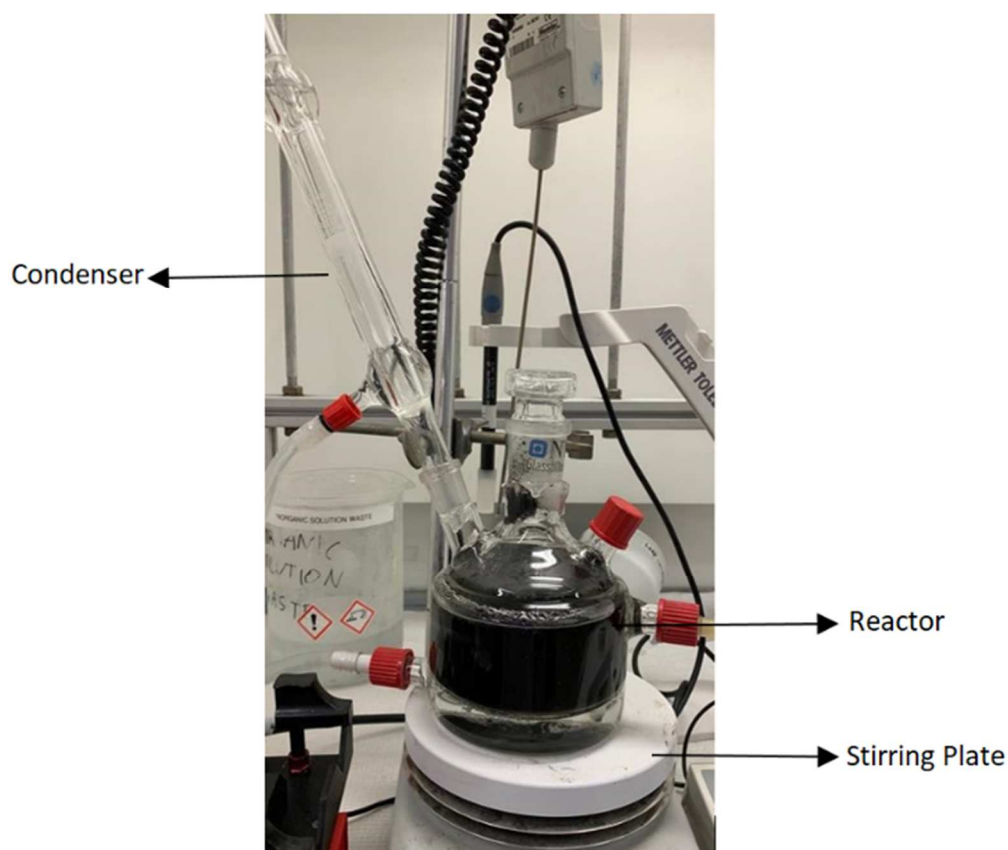


Figure 3.2 - Leaching set-up.

- **Solvent Extraction with D2EHPA:** Solvent extraction experiments were carried in centrifuge tubes (50 ml, polypropylene, VWR). The aqueous phases were the leachates and the organic phase consisted of D2EHPA, TBP and the diluent. Equal volumes of the aqueous and organic phase (10 ml) were added to the centrifuge tubes (O/A=1). The centrifuge tubes were placed in the shaker for 10 minutes. After shaking, the mixture was transferred to the separating funnels and then separated into two phases. Each phase after separation was kept in a vial for future analysis. Fig. 3.3 demonstrates the solvent extraction set-up. The concentrations of used extractant are provided in Table (3.1).

Table 3.1 - Composition of the organic part.

Organics	D2EHPA (mL)	Diluent (mL)	TBP (mL)
10 vol% D2EHPA	1	8.5	0.5
20 vol% D2EHPA	2	7.5	0.5
30 vol% D2EHPA	3	6.5	0.5
40 vol% D2EHPA	4	5.5	0.5

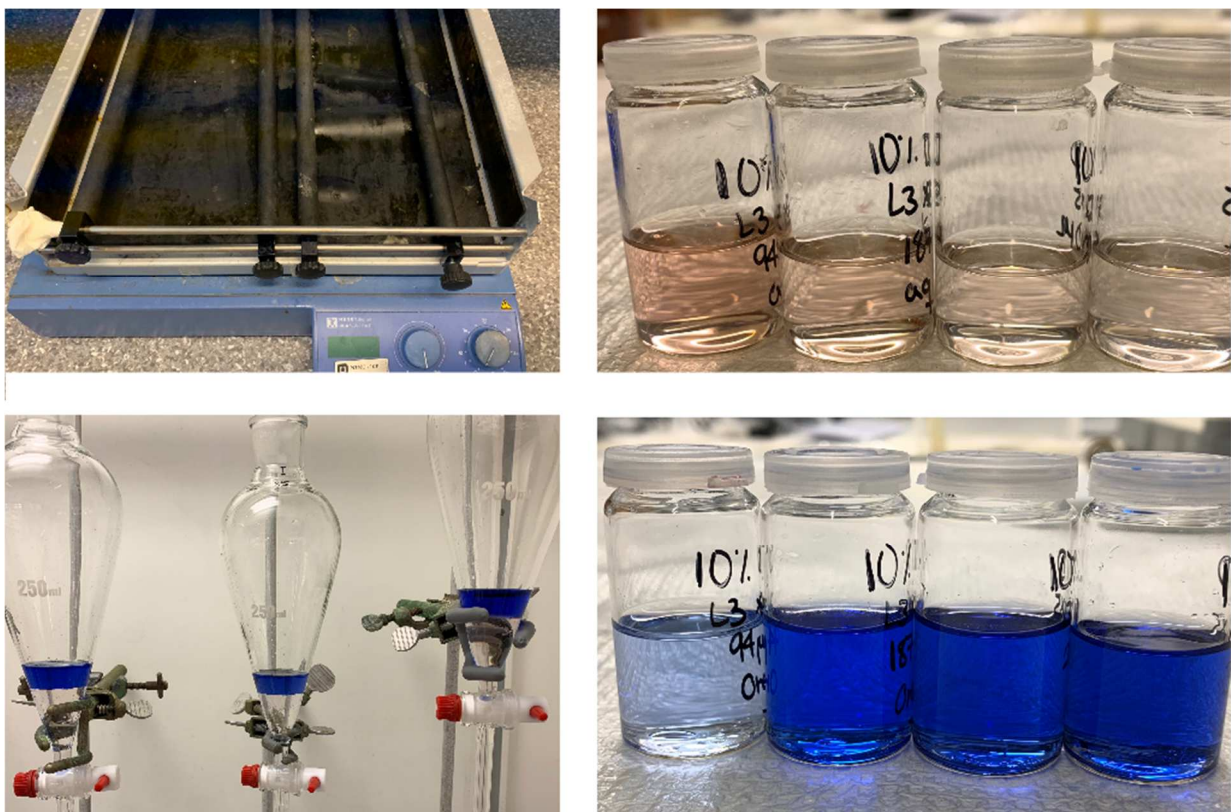


Figure 3.3 - Solvent extraction set-up. Top left is shaker, bottom left is separating funnels, top right is the aqueous phase after separation and bottom right is the organic phase after separation.

- Solvent Extraction with HBTA+TOPO System:** Solvent extraction experiments were conducted in centrifuge tubes (50 ml, polypropylene, VWR), and the organic and aqueous phases (obtained by wet-crushing of batteries) were mixed for 6 minutes in the shaker. The aqueous feed was different concentrations of wastewater, and the organic phase was composed of 0.4 M HBTA + 0.4 M TOPO. The O/A was equal to one and the experiments were carried out in room temperature. Each set of experiments was repeated three times. Fig. 3.4 exhibits the organic and aqueous part after separation.

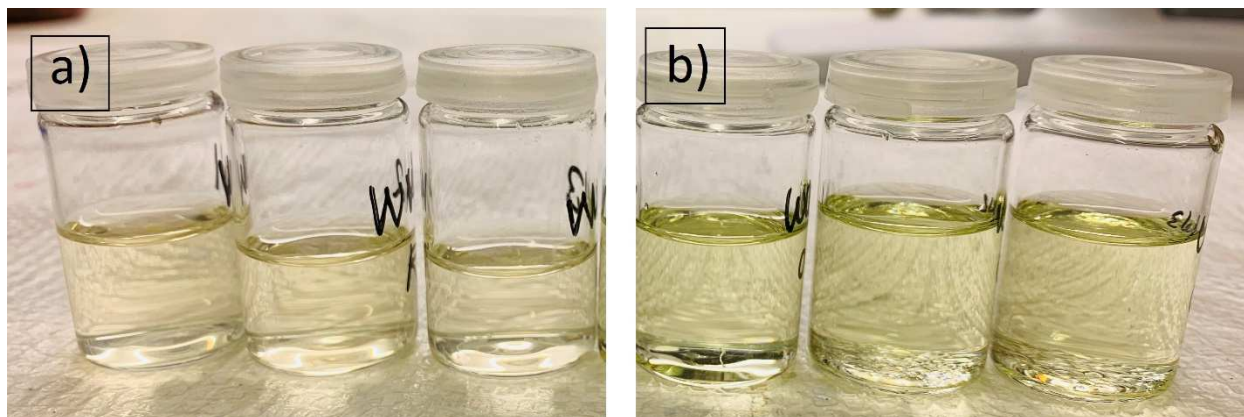


Figure 3.4 - a) the aqueous phases and b) the organic phases after extraction with HBTA+TOPO.

3.2 Characterization Equipment:

In this sub-chapter, characterization methods that was used during the project will be explained.

3.2.1 X-ray Fluorescence Spectroscopy (XRF):

X-ray Fluorescence spectroscopy (XRF) is a non-destructive characterization method. XRF is a straightforward method to determine the elemental composition. In addition, XRF can be used for a wide range of elements, from sodium to uranium. The detection limit for XRF is from part per million (ppm) to high weight percentage (wt.%). In the XRF, the sample is hit with the photons of sufficient energy, and they could be generated by an x-ray tube. These photons can eject the electrons from their orbit to eject the electrons; the energy of photons ($h\nu$) should be higher than the energy that bound electrons to the nucleolus of an atom. When the electron was ejected from the inner orbital, other electrons from the higher orbital will fill the free spot in the inner orbital. Since there is an energy difference between two orbitals, the transfer photon can be emitted from the atom. These fluorescence rays are called characteristic X-ray of the element [34].

The energy difference between two specific orbitals is always the same for a given element. The photon emitted during the transfer between two orbitals will always have the same energy. Therefore, by determining the X-ray photon's energy or wavelength emitted by a specific element, it is possible to determine the identity of that element. There are two types of XRF, wavelength dispersive XRF (WDXRF) and energy dispersive XRF (EDXRF). WDXRF has a higher sensitivity than the EDXRF and works based on Bragg's law (similar to XRD). The amount of specific

elements in a sample is determined by counting the photons of a particular wavelength or energy per unit of time. These fluorescence x-rays form peaks in a semi-Gaussian distribution, and peak intensity is related to the sample element's abundance [34].

XRF was used as a quantitative characterization technique for the preliminary experiments on CoSO_4 synthetic solution. Due to some limitations, XRF was not an applicable characterization method for more complex media such as leachates. The most important one is the inability to detect Li since XRF gives elemental analysis from oxygen (atomic number 8) to uranium (atomic number 92) [35]. Also, fluorescence x-rays of some elements overlap, and therefore some elements show up in the results that are not present in the actual sample. However, it is possible to calculate relative compositions or ratios, such as extraction efficiencies.

3.2.2 Microwave Plasma-Atomic Emission Spectrometer (MP-AES):

Atomic emission spectroscopy is an essential instrumental technique for quantitative analysis of metallic and non-metallic elements in inorganic and organic materials. The AES method involves two steps; first, a sample is atomized in a sufficiently hot source to produce an excited-state species that will emit radiation upon relaxation back to the ground state. Secondly, the radiation that is created is measured at distinct wavelengths by a high-resolution spectrometer. A wide variety of sources exist for the production of excited-state atoms or ions in AES. These sources include flames, plasmas, arcs, sparks, and lasers. Ideally, a source should have some essential characteristics. It should create a high temperature to atomize and excite as many elements as possible, operate in a chemically inert environment such as a nitrogen environment, and analyze solid, liquid, or gaseous samples, possess a low background noise and produce accurate results. The one source with all the mentioned characteristics is the plasma sources such as microwave plasma (MP) sources. The atoms are excited by plasma and emit light at characteristic wavelengths. Then the emissions from each element will be directed to the monochromator. Monochromator should have a sufficient resolution to separate closely spaced elemental emission lines and background lines. Then a high-efficiency CCD (charge-couple device) detector collects all the emissions that filtered through the monochromator. MP-AES quantifies the concentration of an element by comparing the intensity of its emission line to known concentrations of the

element. Therefore, MP-AES needs calibration solutions and curves in order to quantify the concentrations [36].

3.3 Methodology:

In this chapter, all the procedures that carried out will be explained in details.

3.3.1 X-ray Fluorescence (XRF):

XRF was carried out using Rigaku Supermini 200 (WDXRF). This instrument can analyze solids, liquids, alloys, thin films, and powders. The atmosphere can be varied from air, vacuum, and helium. There are two types of detector, PC detector, and scintillation detector. Analyzing liquid samples using XRF is simple, and no sample preparation is needed. For liquid samples, the atmosphere needs to be set to helium. Polypropylene film (P.P. film) was used in sample holder for all liquid samples. Since polypropylene has good resistance towards acids, it is the best film that can be used for acidic samples. The film was used as the sample holder's base, and a sufficient amount (only to cover the P.P. film) of liquid was poured into the sample holder using disposable pipets. Then the samples were put into the equipment and the data obtained in a mass percentage.



Figure 3.5 - Rigaku Supermini200 [35].

The extraction efficiencies ($E\%$) for cobalt from the synthetic leachate calculated based Equation (3.1).

$$E\% = \frac{[Mass\% Co]_{before\ extraction,aq} - [Mass\% Co]_{after\ extraction,aq}}{[Mass\% Co]_{before\ extraction,aq}} \cdot 100 \quad (3.1)$$

3.3.2 Microwave Plasma-Atomic Emission Spectrometer (MP-AES):

MP-AES was carried out using Agilent 4210. MP-AES is more accurate than XRF, it can analyze Li, and gives each element's concentration in ppm [37]. As mentioned in Ch. 3.2.2, MP-AES needs calibration solutions; therefore, 5 calibration solutions with concentrations of 1, 2.5, 4, 5, and 10 mg/L of desired elements, were prepared before analyzing the samples. The calibration solutions were obtained by diluting the multi-element standard solution (Ag, Al, B, Ba, Bi, Ca, Cd, Co, Cr, Cu, Fe, Ga, In, K, Li, Mg, Mn, Na, Ni, Pb, Sr, Tl, Zn, Centipur®, Merck). Since the calibration solutions' maximum concentration is 10 mg/L, the samples need to be diluted 1000 times in order to their concentrations lie in the calibration curve. To validate the accuracy of the MP-AES, calculated amounts of MnSO₄, CoSO₄, NiSO₄, and CuSO₄ were dissolved in DI water to prepare four different synthetic solutions. Then each solution was diluted 1000 times, and then the elemental composition of solutions was measured by MP-AES. Fig. 3.6 shows the theoretical (calculated) and actual (measured by MP-AES) concentration of each element in the synthetic leachates, and the regression line equation. Fig. 3.7 demonstrates the Agilent 4210 instrument.

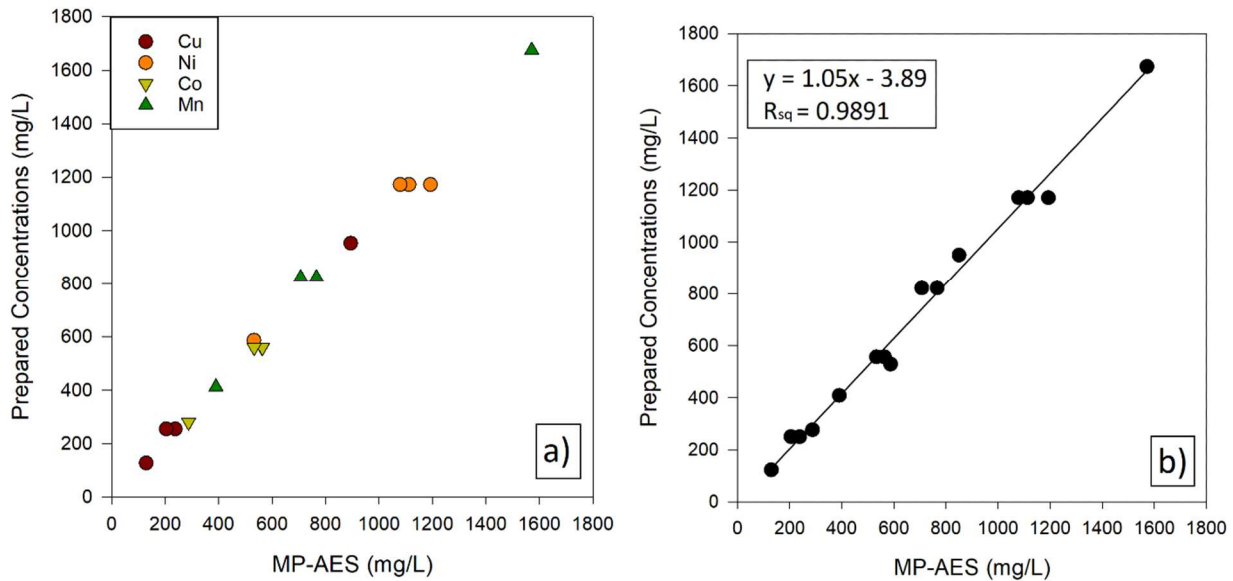


Figure 3.6 – a) Prepared concentration vs concentrations obtained by MP-AES, b) regression line equation.



Figure 3.7 - Agilent 4210 instrument [37].

3.3.3 Solvent Extraction

- **Solvent Extraction on Synthetic Solutions with D2EHPA:** Synthetic solutions were made by dissolving a stoichiometric amount of CoSO_4 , NiSO_4 , MnSO_4 , and CuSO_4 powders in DI water. The pH of the synthetic solutions was 5.3; therefore, a further adjustment was not needed. 40% D2EHPA is equal to 0.012 moles of D2EHPA (D2EHPA density = 0.965 g/mL and D2EHPA molecular weight = 322.42 g/mol). Saponification of the organic phase was done by adding 25 wt.% ammonia. Reaction (3.1) demonstrates the saponification reaction.



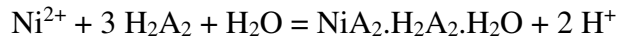
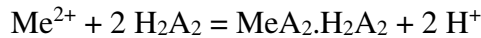
Based on Reaction (3.1), 0.012 moles of NH_4OH is needed to fully saponify D2EHPA. Hence, 1870 μL of 25 wt.% ammonia is needed to fully saponified D2EHPA. For example, 20% saponification means adding 375 μL of 25 wt.% ammonia to the organic phase.

A calculated amount of ammonia was added to the organic phase and stirred for 10 minutes. For all the experiments, O/A was equal to 1. For experiments with synthetic CoSO_4

solution, the aqueous part after separation of two phases was analyzed by XRF, and the E% was calculated based on Equation (3.1). However, it is better to use MP-AES for more complex media; therefore, for the synthetic solutions containing all the four metal ions, MP-AES was used for analyzing the aqueous part after the separation of two phases. Distribution coefficient (D) and extraction efficiency (E%) were calculated based on Equation (3.2), where [Me] stands for metal ions.

$$D = \frac{[Me]_{org}}{[Me]_{aq,after\ extraction}} \quad E\% = \frac{100D}{D + 1} \quad (3.2)$$

- Solvent Extraction on Leachates with D2EHPA:** For leachates, 25 wt.% ammonia was added drop by drop using 100 -1000 μ L pipettes till leachate pH adjusted to 5.5. In order to obtain a precipitate-free and transparent solution, the leachates were filtered. For filtration, a filter paper with 0.22 μ m of pore diameter (Durapore® PVDF Membrane, Merck) was used. Saponification of the organic phase was done the same way as explained above. Distribution coefficient (D) and extraction efficiency were calculated based on Equation (3.2). The chemical reaction presented below was used to calculate the D2EHPA loading percentage [21][22][33][38]. “Me” stands for Co, Mn, Li and Cu. Each of these elements react with 2 moles of D2EHPA. However, Ni reacts with 3 moles of D2EHPA [21]. Al was not included in the calculation since its concentration was low. D2EHPA loading percentage was calculated using Equation (3.3).



$$D2EHPA\ loading\ percentage = \frac{\sum n_{Mn,Co,Li,Cu} \cdot 2 + n_{Ni} \cdot 3}{n_{D2EHPA}} \quad (3.3)$$

The Equation (2.7) in Ch. 2, was used to calculate the separation factor (β) of Mn over other metal ions.

- **Solvent Extraction with HBTA+TOPO:** The aqueous feed was the wastewater that was obtained from the wet-crushing of the batteries, the procedure of wet-crushing was explained in Ch. 3.1.2. Wastewater pH was adjusted to 9.5 by adding drop by drop of 5 M NaOH solution [6], then it was filtered. For filtration, a filter paper with 0.22 μm of pore diameter (Durapore® PVDF Membrane, Merck) was used. In order to study the effect of Li concentration on E%, after filtration, the wastewater was up-concentrated to get a higher concentration of Li. Up-concentration was done by heating up 300 mL of wastewater for 2h until the volume was smaller than 100 mL. It was then transferred to a 100 mL volumetric flask, and DI water was added to reach the 100 mL.

The organic phase was composed of 0.4 M HBTA + 0.4 M TOPO. 0.8 M HBTA in kerosene and 0.8 M TOPO in kerosene were made separately in 50 mL volumetric flasks. 8.64 g of HBTA was melted at 38 C in the volumetric flask, then kerosene was added to the designated volume. 15.46 g of TOPO was melted at 52 C, and kerosene was added to the volumetric flask. 5 mL of HBTA was saponified by adding 560 μL of 5 M NaOH (70% saponification) solution and stirred for 5 minutes. After that, 5 ml of TOPO was added to 5 ml of saponified HBTA. 9.5 mL of wastewater water was mixed with the organic part to keep the O/A=1. Each set of experiments was repeated three times.

4 Results and Discussion

In this chapter, results obtained from the experiments will be discussed thoroughly. The first five chapters are focused on the extraction and separation of metal ions from leachates using D2EHPA as an organic solvent. The last chapter is focused on the extraction of Li from wastewater using HBTA as an organic solvent.

4.1 Preliminary Studies on CoSO_4 Synthetic Solution

In order to study the extraction behavior of Co using D2EHPA, preliminary studies on synthetic CoSO_4 were done. Effects of D2EHPA concentration, the addition of TBP to the organic phase, Co concentration, and saponification of the organic phase were investigated.

4.1.1 Effect of D2EHPA Concentration in the Organic Phase

To investigate Co extraction using D2EHPA, extraction experiments were conducted with CoSO_4 synthetic solution. The Co concentration in the synthetic solution was 0.001 M and the pH was 5.3. D2EHPA concentrations was varied in the organic phase (10 to 40 vol%) in Asol D80. XRF was done on the aqueous phases after separation to determine the elemental composition of the aqueous phase after extraction, as it mentioned in Ch. 3, XRF was used for simple synthetic solutions that only contain Co. With an increase in D2EHPA concentration in the organic phase, there is an increase in extraction efficiency, see Fig 4.1.a. Based on equation (2.5) in Ch. 2, higher concentration of D2EHPA also leads to higher distribution coefficient (D) and higher extraction efficiency (E%). Higher concentration of D2EHPA means there are more molecules of D2EHPA are available for formation of Co tetrahedral complex in the organic phase. However, the efficiencies are relatively low, which could be due to the low equilibrium pH (=2.3)

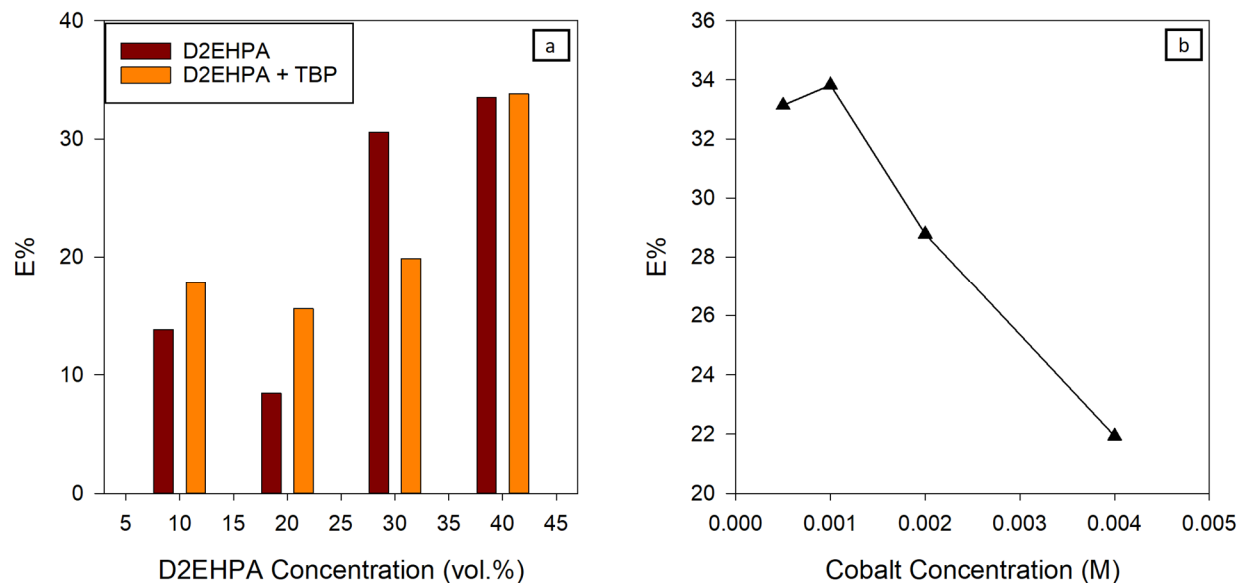


Figure 4.1 - E% as a function of D2EHPA concentration, b) effect of initial Co concentration.

4.1.2 Effect of TBP Additions to the Organic Phase

The extraction experiments were conducted with 0.001 M CoSO_4 as the aqueous feed and a combination of D2EHPA, TBP, and Asol D80 as the organic phase. Fig. 4.1.a demonstrates with the addition of TBP to the organic phase, the E% of Co increased. TBP by itself can not extract Co from sulfate media. The role of TBP is to disrupt the dimers or aggregation of the D2EHPA molecules. TBP can bridge with acidic extractant D2EHPA through the lone electron pair available from its phosphorus–oxygen (P=O) bond [39]. Therefore, the addition of TBP can enhance the extraction by providing more D2EHPA molecules available for the formation of the cobalt tetrahedral in the organic phase.

For 40 vol% D2EHPA adding 5 vol% of TBP did not make a difference in extraction efficiency since TBP concentration is low compared to D2EHPA concentration. Therefore, there are not enough TBP molecules available to depolymerize the dimers of D2EHPA. Contrary to previous studies, for 30 vol% of D2EHPA, adding TBP led to decrease in extraction efficiencies. That can be due to the less accuracy and uncertainty of the characterization method. Based on a study by Manousakas et al. [40] XRF average uncertainty for Co is 20%. Liquid XRF gave a general overview of aqueous phase elemental composition, but it is not accurate. Hence, some errors should be accepted.

4.1.3 Effect of Cobalt Concentration

Based on the result of previous experiments, 40 vol% D2EHPA was chosen for further experiments. The effect of different Co concentration on E% was studied, using 40 vol% D2EHPA and 5 vol% TBP in Asol D80 as the organic phase. Fig. 4.1.b exhibits that with higher cobalt concentrations, extraction efficiency decreased. Based on equation (2.2) in Ch. 2, a higher metal ion concentration will decrease K_{ex} . Lower K_{ex} will result in a lower D and therefore lower E%. Based on the reaction (3.1) in Ch. 3, two moles of D2EHPA should react with 1 mole of cobalt ion, and there are 0.012 moles of D2EHPA available in the organic phase; therefore, it can extract up to 0.006 moles of cobalt from the aqueous phase. It can be seen from the experimental data that the D2EHPA could not use its maximum loading capacity, and extraction efficiency is still low. As mentioned in Ch. 2 and equation (2.5), equilibrium pH plays a vital role in extraction since the extraction abilities of D2EHPA is closely related to the equilibrium pH. In lower equilibrium pH, the extraction of Co from sulfate media is low [41][42][39]. Therefore, to increase the E%, the equilibrium pH should be increase.

4.1.4 Effect of Saponifying the Organic Phase

It is feasible to increase the equilibrium pH for extraction in two different ways, either saponify the organic phase or increase the aqueous feed solution's pH. It is impossible to increase the aqueous phase's pH to higher than 8 since Co will start to precipitate around pH=8 [39]. Therefore, the other option is to saponify the organic phase. Bases such as NaOH and ammonia can be used for saponification of the organic phase. By adding these bases to acidic extractant, part of the extractant neutralized. The neutral form of the extractant exists as a monomer hence, there are more molecule of extract are available to form the cobalt tetrahedral. The reaction (4.1) describes the neutralization of D2EHPA using ammonia, it is similar to reaction (2.7) in Ch. 2, but NaOH was replaced by ammonia:



As mentioned in Ch. 3.3.3, in order to saponify 40 vol% D2EHPA, 1870 μ L of 25 wt.% ammonia should be added to the organic phase. To examine the changes in pH of the organic phase after adding ammonia, 25 wt.% ammonia was added to the organic phase, and then the pH of the organic

phase was measured. It should be noted that pH measurements in the organic phase could be uncertain since the pH electrode is made for aqueous solutions, the following numbers could be uncertain. The results are presented in Fig. 4.2.

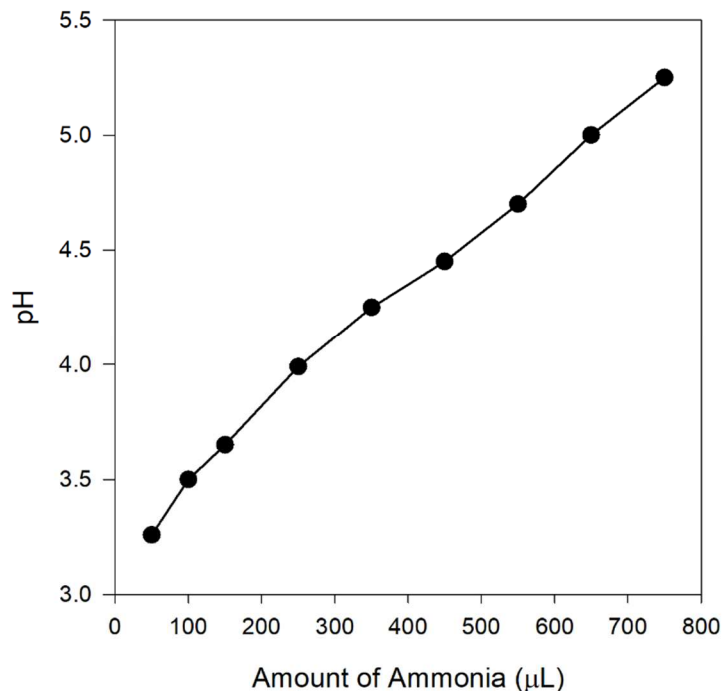


Figure 4.2 - Effect of ammonia volume on pH of the organic phase.

When D2EHPA was saponified 40% (equal to 750 µL of added ammonia), the mixture after shaking became cloudy and separation took a long time, 24h. The cloudiness and time-consuming separation were never reported in previous studies where Kerosene was used as a diluent [43][22]. However, in the current study, Asol D80 was used as diluent and that could be the reason for the long separation time and the cloudiness of the mixture after adding 750 µL of ammonia. Fig. 4.3 exhibits the cloudiness of the aqueous part after separation when higher volume of ammonia was used. Lower volumes of ammonia were added to the organic phase for further experiments, which means lower saponification percentage, to decrease the separation time.

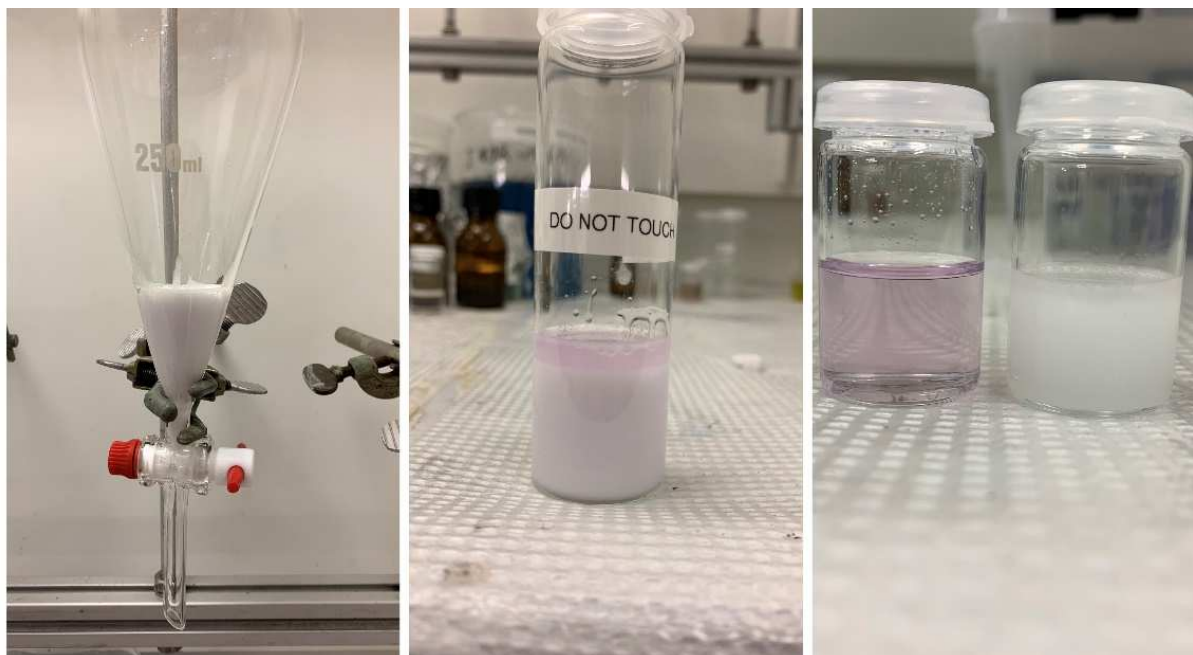


Figure 4.3 - Picture on left demonstrate the mixture of the organic and the aqueous phase after shaking, picture on middle shows the mixture after 6h and picture on the right exhibits the organic phase and the aqueous phase after separation.

For this experiment set, D2EHPA was saponified 10%, 15%, and 20% by adding calculated volumes of 25 wt.% ammonia to the organic phase. The aqueous phase was 0.001 M cobalt sulfate solution and the extraction condition was the same as in the previous experiments. After separation, the aqueous parts were analyzed by XRF. There was no Co detected, in the XRF detection range, in all the aqueous phases after separation. Fig. 4.4 represent E% of Co as function of saponification percentage. Before saponification of the organic phase, the equilibrium pH of the aqueous phase after extraction was 2.3. However, after saponification of the organic phase, the equilibrium pH was 4.2 or higher. It has been shown in the previous studies that Co extraction efficiency using D2EHPA as organic solvent reaches close to 100% in pH=4 [42]. Since the number of moles of available D2EHPA is higher than the number of Co moles, even a low saponification rate can lead to 100% extraction efficiency.

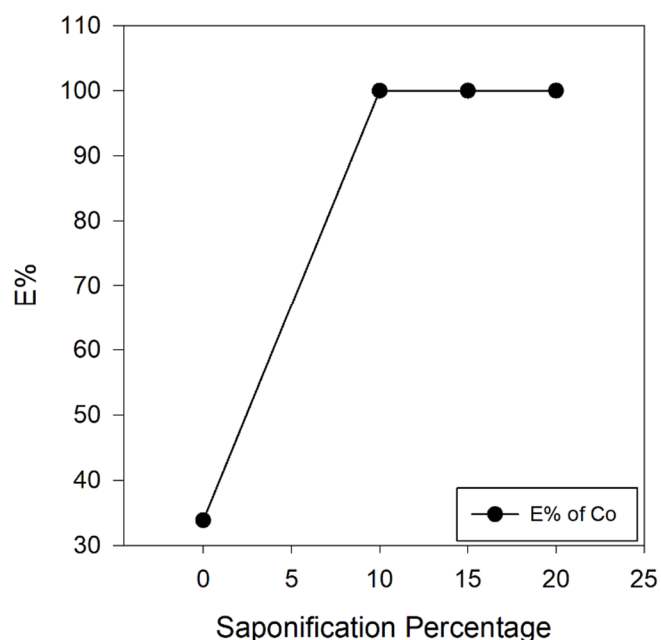


Figure 4.4 - E% of Co as a function of saponification percentage.

A higher saponification rate is needed for more concentrated solutions such as leachates from battery leaching. However, a higher saponification rate such as 80% and above will lead to higher pH in the interference of two phases. An equilibrium pH of higher than 8 will lead to the formation of cobalt hydroxide or other metal hydroxides in the organic/aqueous interface [39]. These solid hydroxide particles can interrupt the mass transfer of metal ions from the aqueous phase to the organic phase and then hinder the extraction process. Considering the separation time and optimum equilibrium pH, 20% saponification rate was chosen for the next series of experiments.

4.2 Preliminary Study on Synthetic Solutions Containing MnSO_4 , CoSO_4 , CuSO_4 , and NiSO_4

In order to study the extraction mechanism in multi-ion aqueous feed, four different synthetic leachates were made, see Table 4.1. Synthetic leachates are less complex version of the leachates since their condition such as concentration of elements, presence of impurities, and unwanted complexes, can be easily controlled. The first synthetic leachate has a low Co concentration compared to Mn and Ni, therefore one can see how D2EHPA extract Co when the concentration of Mn is higher. Both Co and Mn has a strong affinity towards D2EHPA [43]. The second one has

the same concentration for Co and Ni while the concentration of Mn was doubled. Synthetic leachate III will show the extraction order when Cu has a higher concentration than Mn. Synthetic leachate IV has a lower concentration of Co and Ni, while Cu and Mn concentrations are the same as for leachate I. For these experiments, the organic phase was saponified by 25 wt.% ammonia, and the saponification percentage was 20%. The aqueous feed solution was each of the synthetic leachates with a pH ranging from 5.1 to 5.6.

Table 4.1 - Elemental composition of the synthetic leachates, measured by MP-AES.

Element	Cu (mg/L)	Ni (mg/L)	Co (mg/L)	Mn (mg/L)
Synthetic Leachate I	237.86	1112.45	562.14	765.75
Synthetic Leachate II	128.91	1193.96	563.35	1571.21
Synthetic Leachate III	849.33	1079.04	532.74	389.55
Synthetic Leachate IV	204.19	532.2	287.29	706.36

Fig. 4.5 demonstrates the E% for each element. The elemental composition of each aqueous feed after extraction, D, and E% can be found in Appendix. All the metal ions present in synthetic leachates were extracted, and extraction efficiency for each element was 96% and higher. The extraction order for D2EHPA is $Mn^{2+} > Cu^{2+} > Co^{2+} > Ni^{2+}$ [43]. In synthetic leachate II with the highest Mn concentration, Mn's extraction efficiency is the highest. D2EHPA has a high affinity towards Mn; therefore, it can extract most of the Mn present in the aqueous phase. Since the concentration of Mn is the highest between the other leachates, most of available D2EHPA molecules were formed a complex with Mn and extract Mn first; therefore, there are less D2EHPA molecules available for Cu extraction.

Fig. 4.5 also exhibits that Co extraction efficiency is 100% in all four synthetic leachates because Co concentration is low compared to Mn and Cu. Additionally, the number of Cu and Mn moles

is lower than the available D2EHPA moles. Hence, D2EHPA has some capacity left to extract Co fully; also, the same logic applies for Ni. D2EHPA still has some capacity left to extract Ni after extracting all the other metal ions. Synthetic leachate IV has the lowest metal ion concentration; therefore, all of them are extracted with extraction efficiency equal to 100.

As it mentioned above, the main reasons that can cause such a high extraction efficiency for all the present elements is high D2EHPA concentration. The maximum amount of metal ions available in the synthetic leachates are 0.0006 moles which is only 10% of the loading capacity of D2EHPA, therefore D2EHPA can extract all the metal ions with high efficiency. However, the concentration of metal ions in the leachates are higher than these synthetic leachates (10 times higher). Therefore, in order to study D2EHPA extraction order in the leachates, which is a more complex media, 40 vol% D2EHPA was used for the further experiments.

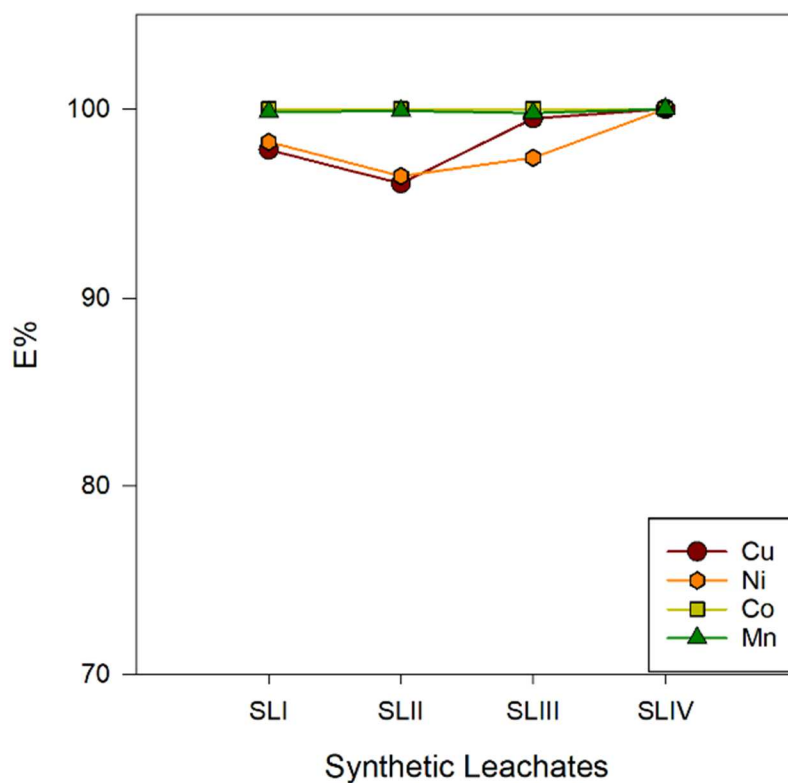


Figure 4.5 - Extraction efficiency of each element in different synthetic leachate.

4.3 Study of D2EHPA Extraction Mechanism on Leachate

4.3.1 Effect of Initial Concentration of Each Element on E%

Four different leachates were chosen for these experiments. The leachates were diluted 5 and 10 times, and the pH was set to 5.3-5.5 by using 25 wt.% ammonia. After changing the pH, the leachates become cloudy; therefore, filtration was done to obtain a transparent solution. Elemental composition of the aqueous phases before and after extraction were determined by MP-AES. Table (4.2) represent the elemental composition of each leachate without dilution. The 5 and 10 times diluted leachate and the aqueous part after extraction's elemental compositions can be find in the Appendix.

Table 4.2 - Elemental composition of different leachates, measured by MP-AES.

Element	Cu (mg/L)	Ni (mg/L)	Co (mg/L)	Li (mg/L)	Mn (mg/L)	Al (mg/L)
S/L=95	677.75	4233.69	4257.57	1438.84	3390.23	77.12
S/L=120	1045.65	5276.23	5751.56	2177.43	4670.38	130.61
S/L=95E	215.12	2401.53	2371.19	796.30	1935.72	19.82
S/L=120E	265.80	2875.89	2990.45	994.16	2392.75	24.16

The organic phase was saponified 20% by 25 wt.% ammonia. After mixing and separating, D, and E%, for each element were calculated. In order to study the extraction order of D2EHPA, 40% D2EHPA was used. Fig. 4.6 represents E% of each element as a function of each element concentration. Table (4.3) presents the equilibrium pH for each set of experiment.

Table 4.3 - Equilibrium pH for each set of experiments.

Exp.	pH_{eq}	Exp.	pH_{eq}	Exp.	pH_{eq}	Exp.	pH_{eq}
S/L=95	3.5	S/L=120	3.5	S/L=95E	3.6	S/L=120E	3.7
S/L=95,x5	4.2	S/L=120,x5	4.2	S/L=95E,x5	4.2	S/L=120E,x5	4.2
S/L=95,x10	4.3	S/L=120,x10	4.3	S/L=95,x10	4.3	S/L=120E,x10	4.4

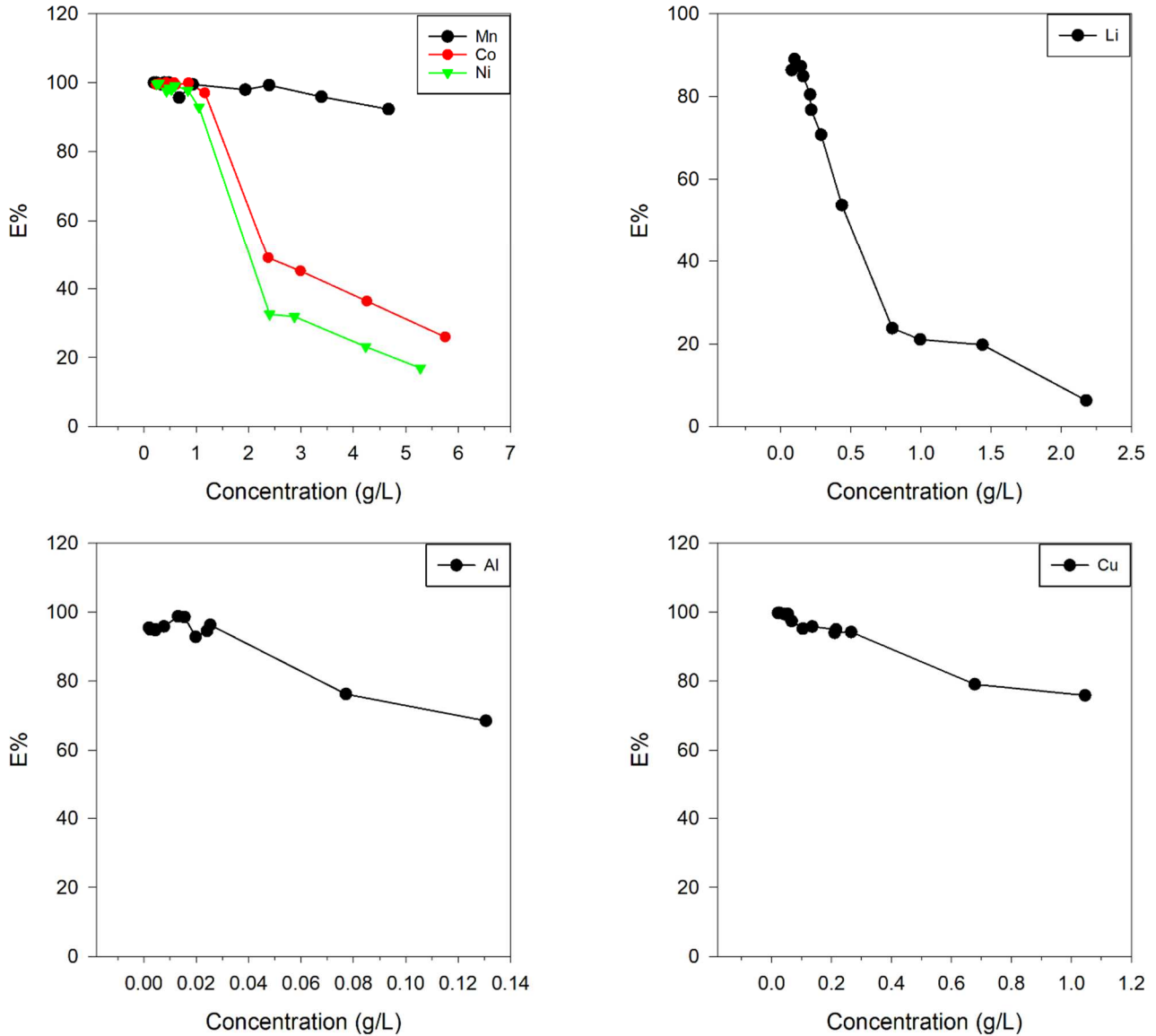


Figure 4.6 - E% as a function of concentration of each element (g/L).

Based on Fig. 4.6, the E% of Mn does not depend strongly on its initial concentration in the aqueous feed. No matter what concentration Mn has, E% of Mn is always close to 100%. E% of Cu is high in the lower concentration and decreased 24% when Cu's initial concentration was the highest. Al has the same behavior as Cu, but the decrease in the E% was higher than Cu. The other elements follow the same trend as Cu, and Al. However, their E% decreased significantly when their concentration increased and the decreasing trend in E% is more notable for Li.

The aqueous feeds are leachates obtained from the leaching of the NMC (1:1:1 ratio between Mn, Co, and Ni) prismatic battery cells; therefore, whenever Mn's concentration is high in the leachates, Co and Ni's concentration is also high. Since D2EHPA has a higher affinity towards Mn and Cu [31][42], it extracts Mn and Cu first. Then it extracts Co and then Ni, and by that time, D2EHPA is saturated with Mn and Cu; hence, there are fewer D2EHPA molecules available to extract Co and Ni. In the case of Li, Li is the last metal ion that extracts from the aqueous feed. When other ions have high concentrations, D2EHPA is saturated with those divalent and trivalent ions. Therefore, there are fewer available extractant molecules for Li extraction.

Al and Cu are impurities from batteries foil. As mentioned above, D2EHPA has a higher affinity towards Cu than Co, Ni, or Li. Moreover, the initial concentration of Cu in the leachates is always lower than Co and Ni, therefore the decrease in E% of Cu is lower than decrease in E% of Co, and Ni. The small decrease in E% of Cu in higher concentration is because when the Cu concentration is high, Mn concentration is also high, and since D2EHPA has a higher affinity towards Mn, D2EHPA extracts Mn first, and then Cu. Therefore E% of Cu is started to decrease when the concentration of Mn increased. Al is a trivalent ion; therefore, it co-extract with other divalent ions and since Al concentration is low in the leachates, E% of Al is relatively high.

When the concentration of all the elements are low, such as diluted leachates, the E% is high for all of them. Therefore, D2EHPA does not show any selectivity towards any metal ion, which could be due to high D2EHPA concentration (1.2M). High D2EHPA concentration will lead to high enough loading capacity for D2EHPA to extract all the metal ions from the aqueous feed.

Previous studies such as a study by Hu et al. [32] separate a divalent ion (calcium) from Ni by D2EHPA, and only 1% of Ni was co-extracted. They used 10 vol% D2EHPA for extraction, and Ni content was relatively high (89 g/L of Ni and 0.6 g/L of Ca). The equilibrium pH was 2.5, and it was lower than any equilibrium pH for experiment sets in this current study. In another study by Li et al. [22], they recover Mn from leachates of spent LIBs by 15 vol% D2EHPA in kerosene. The aqueous feed in the mentioned study consisted of 7.2 g/L Li, 8.5 g/L Mn, 8.1 g/L Co and 6.2 g/L Ni. The equilibrium pH was 1 and O/A=0.5. The two mentioned studies have three conditions: a higher concentration of metal ions in the aqueous feed, lower D2EHPA concentration, and lower equilibrium pH than the current study. Therefore, in order to study the effect of equilibrium pH and D2EHPA concentration on the E% of elements and D2EHPA selectivity, the next series of experiments were conducted.

4.3.2 The Effect of Equilibrium pH on the E%:

Equilibrium pH plays an important role when it comes to the separation of metal ions from each other. In equilibrium $\text{pH} < 3$, Mn can separate from Co and Ni with limited co-extraction of Ni and Co. By increasing equilibrium pH to 3, Cu can separate from Co and Ni, and in equilibrium, $\text{pH} = 3.5$ Co can be extracted and separated from the Ni. In equilibrium, $\text{pH} > 3.5$ Ni starts to extract, although Ni's extraction efficiency is not high. It is hard to separate Mn and Cu from each other since the equilibrium pH for extracting them is close to each other [21]. Therefore, to study the equilibrium pH effect, two different experiments were done on the five times diluted leachates. In the first set (I), the aqueous feed's pH (4 different leachates) was changed to 5.5 by 25 wt.% ammonia, and the organic phase was not saponified. In the second set (II), the aqueous phase's pH remained unchanged, and the organic phase was 20% saponified by 25 wt.% ammonia. Table (4.4) represents equilibrium pH of each experiment.

Table 4.4 - Equilibrium pH of 3 different set of experiments, each contains 4 different leachate.

Exp.	pH _{eq}	Exp.	pH _{eq}	Exp.	pH _{eq}	Exp.	pH _{eq}
S/L=95,x5	4.2	S/L=120,x5	4.2	S/L=95E,x5	4.2	S/L=120E,x5	4.2
S/L=95,x5 (I)	2.2	S/L=120,x5 (I)	2.1	S/L=95E,x5 (I)	2.2	S/L=120E,x5 (I)	2.2
S/L=95,x5 (II)	3.0	S/L=120,x5 (II)	3.0	S/L=95,x5 (II)	3.1	S/L=120E,x5 (II)	3.2

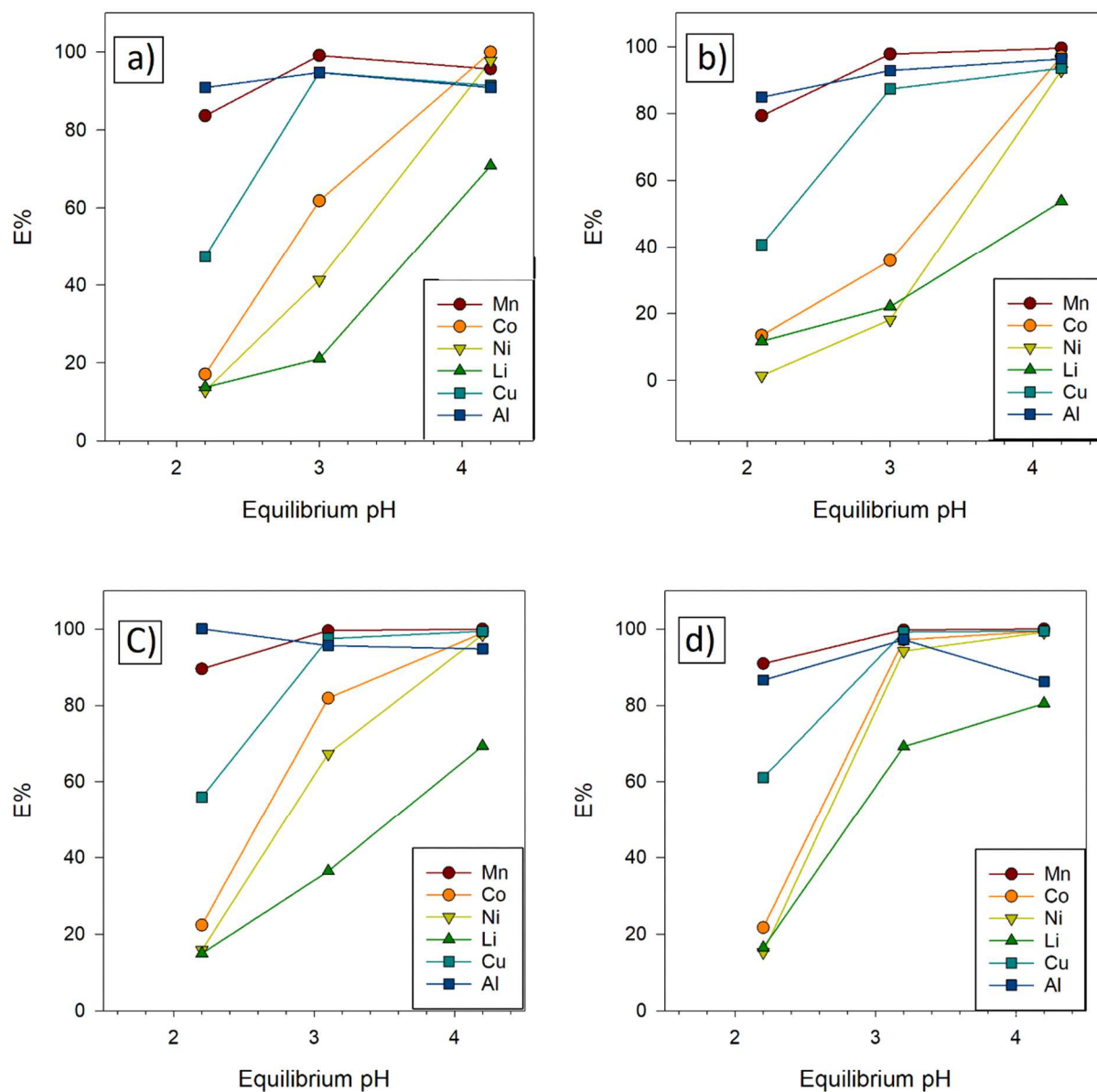


Figure 4.7 - Effect of equilibrium pH on the E%. a) Leachate S/L=95, b) Leachate S/L=120, c) Leachate S/L=95E, d) Leachate S/L=120E.

Fig 4.7 represent the E% of each element as a function of the equilibrium pH. It is clear that with a higher equilibrium pH, the E% for all the elements will increase. Fig. 4.7 demonstrates that in higher equilibrium pH, the E% for all the metal ions are high; therefore, D2EHPA loses its selectivity. In lower equilibrium pH, D2EHPA is more selective towards Mn than Co. Hence, at low equilibrium pH, D2EHPA can selectively extract Mn from the leachates [43]. Based on previous studies [22][42], Mn has high efficiency (close to 90%) in equilibrium pH<3. However,

based on the Fig. 4.7, Mn efficiency is lower in pH=2.2 than pH=3.0-3.2 or pH=4.2 because equilibrium pH=2.2 was obtained when the organic phase was not saponified. As mentioned in Ch. 2, saponification depolymerize D2EHPA into monomers; therefore, there are more D2EHPA molecules are available for extraction. Without saponification, D2EHPA is in its dimer form. Thus, the extraction efficiency for Mn is lower than when D2EHPA was saponified.

4.3.3 D2EHPA Loading Percentage as a Function of Initial Concentration of Metal Ions in Leachate

As mentioned in Ch. 3.3., the D2EHPA loading percentage was calculated for all the leachates and their dilutions. Based on Fig. 4.8, it is clear when the concentration of metal ions in leachates increased, the loading percentage increased. However, even with the most concentrated leachates, D2EHPA is only 26.72% saturated. In order to saturate D2EHPA more, either D2EHPA concentration should be decreased, or the initial concentration of metal ions in the leachates should be increased. Also, for the constant D2EHPA concentration and the initial concentration, if the E% of targeted metal ion increased, the loading percentage could be increased.

A parameter that can affect the extraction efficiency and, therefore, the loading percentage, is the diluent. Kerosene is mostly used as a diluent when D2EHPA is the extractant [33][22][44]. Kerosene has a low dielectric constant (1.8) compared to Asol D80 (2.3) [39]. The extraction efficiency increases with the decrease in the dielectric constant and dipole moment of the diluents. That can be explained by the interactions between the extractants with diluents. The extractants have stronger interactions with diluents having a high dielectric constant, resulting in lower extraction efficiency for divalent ions [39]. Therefore, kerosene was used as a diluent for the next set of experiments since it has more compatibility with D2EHPA.

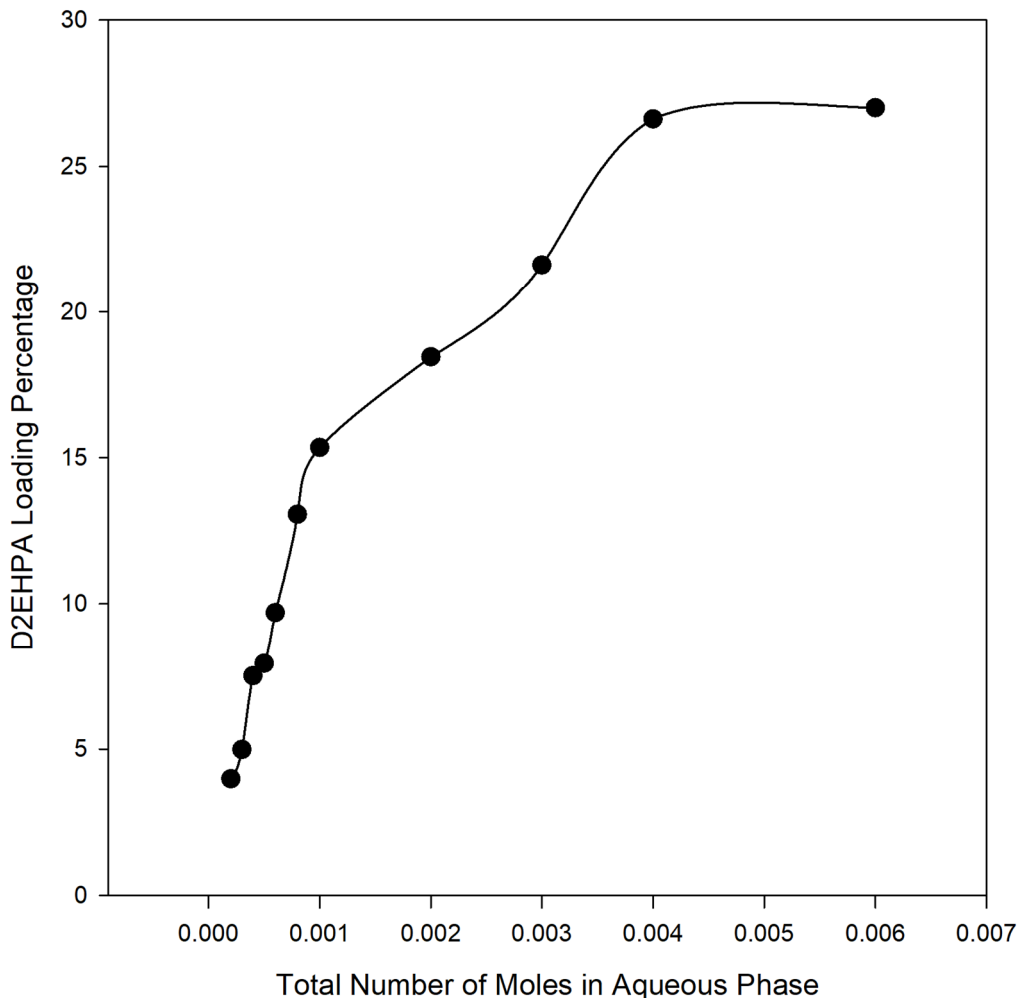


Figure 4.8 - D2EHPA loading percentage vs total number of moles of metal ions in the aqueous phase.

4.4 Selective Extraction of Mn from the Leachates:

Overall goal of this thesis is to separate metal ions from each other in the leachates and based on the presented results, D2EHPA has a high selectivity towards Mn. In order to selectively extract Mn from the leachates, D2EHPA should be saturated with Mn. Although this chapter aimed to investigate the relation between E% of Mn and the D2EHPA loading percentage, the goal was not achieved due to a human error. However, it was revealed that equilibrium pH plays an important role in separating Mn from other elements. 3 different leachates were chosen for the next set of experiments and their elemental composition is presented in Table (4.5). These 3 leachates have a higher concentration of Mn than the previous leachates in Ch. 4.3.1.

Table 4.5 - Elemental composition of different leachates, measured by MP-AES.

Element	Cu (mg/L)	Ni (mg/L)	Co (mg/L)	Li (mg/L)	Mn (mg/L)	Al (mg/L)
L1	2111.45	9284.65	9036.2	3146.55	7310.95	138.45
L2	734.45	8165.05	8000.5	2720.3	6426.5	304.2
L3	1108.7	13791.2	13697.9	4457.15	10800.4	532.15

Each leachate was diluted 2 and 5 times, and then the pH was changed to 5.5 using 25 wt.% ammonia. For the not diluted leachate, when ammonia was added to adjust the pH, the color changed from dark red to dark blue, and a notable amount of precipitates formed in the solution. Due to color change and the volume of precipitates, the extraction was not performed on the leachate without dilution. In the case of 2 times diluted leachate, solid particles were formed after changing the pH to 5.5. However, the amount of precipitates were not as high as the not diluted leachate. Therefore, filtration was done to obtain a precipitate-free solution. After the first filtration step, some green solid particles were left on the filter paper, which could be some metal hydroxides that precipitated at that pH. However, after the first filtration, the solution still contained some small particles. The solution was left overnight and precipitation was still ongoing. Hence a second filtration was performed. As shown in Fig. 4.9, the solution was not precipitate-free even after the second filtration, which could be due to the precipitates' uneven size distribution that raptured the filterability and increased the filtration time [45]. Due to easier filterability, for the extraction experiments, 5 times diluted leachates at pH=5.5 were chosen for the future experiments.



Figure 4.9 - Top left picture shows the change in the color of leachate after adjusting the pH to 5.5 by ammonia, the dark blue is the leachate at pH=5.5. Top right demonstrates the precipitates in the leachate. Bottom left shows the filter cake after filtration of 2 times diluted leachate. Bottom right shows the small precipitates in the leachates after multiple filtration.

D2EHPA concentration was varied in the organic phase, ranging from 10 to 40 vol%, and kerosene was used as a diluent. Due to human error, the same volume of ammonia (375 μL) was added to the organic phase; therefore, the saponification percentage is different for each organic phase. For 10 and 20 vol% D2EHPA, 375 μL of ammonia is equal to 80% and 40% saponification, respectively. However, no cloudiness of the aqueous phase after separation was observed, and

separation of two phases happened in less than 30 minutes (the separation time for 40% saponification was 24h when Asol D80 was used as a diluent, see Ch. 4.1.4). This experiment confirms that the cloudiness and long separation time observed previously with high saponification percentage, such as in Ch. 4.1.4, is likely because of Asol D80. Table (4.6) exhibits the equilibrium pH for different saponification percentage and D2EHPA vol%.

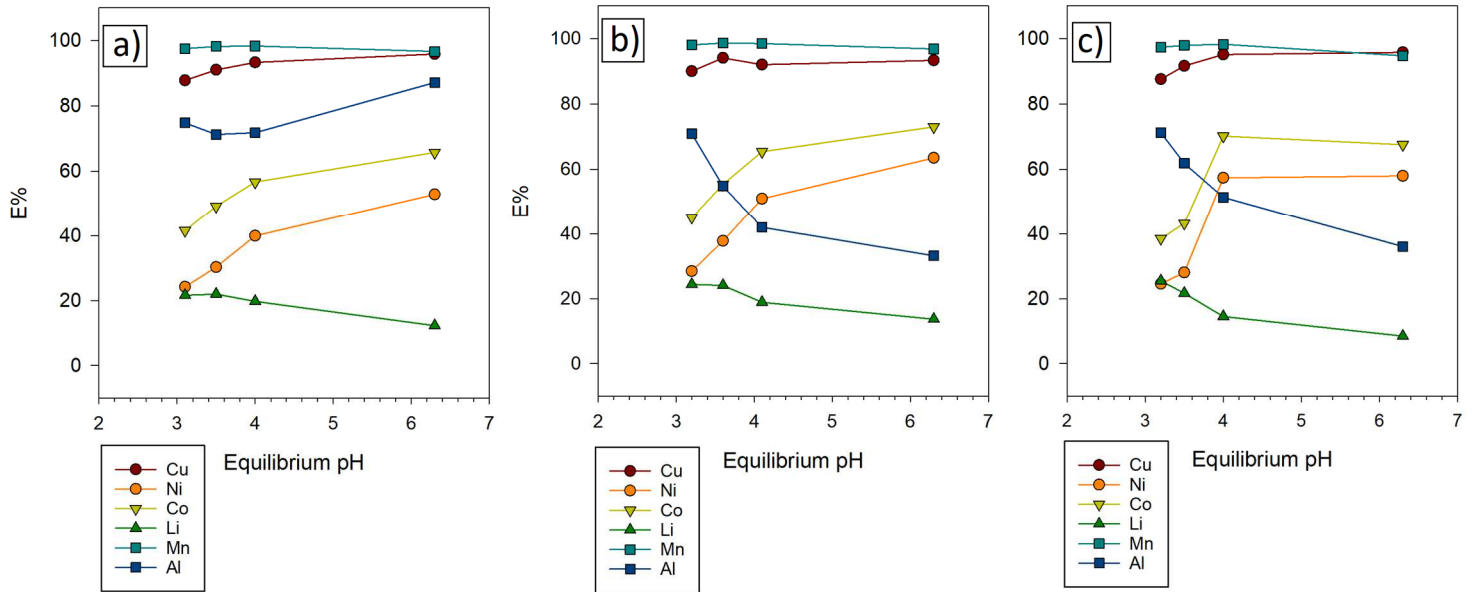


Figure 4.10 - Effect of equilibrium pH on E% when D2EHPA concentration was varied, a) Leachate L1, b) Leachate L2, c) Leachate L3.

Based on Fig. 4.10, when equilibrium pH increased from 3.1 to 6.3, E% for Co and Ni increased. Equilibrium pH=6.3 was obtained when D2EHPA concentration was the lowest. It shows that equilibrium pH has a more significant impact on E% of Co and Ni than D2EHPA concentration. Li extraction efficiency decreased when equilibrium pH increased; therefore, E% of Li is more dependent on the D2EHPA concentration than equilibrium pH. Li is the last metal ion extracted from the aqueous phase; thus, when the concentration of D2EHPA is high, it still can extract Li. However, when the aqueous feed is concentrated and D2EHPA concentration is low, D2EHPA is saturated with other metal ions and can not extract Li. E% for Mn is always close to 100% no matter the D2EHPA concentration or equilibrium pH. Cu has similar behavior to Mn; however,

there is a small increase (<10%) in Cu extraction efficiency with an increase in equilibrium pH. For L2 and L3, E% for Al decreased with an increase in pH, but it was the opposite for L1. Al concentration is low in 5 times diluted L1 (28 ppm); therefore, E% does not affect by equilibrium pH or D2EHPA concentration. Otherwise, Al behavior is similar to Li; D2EHPA concentration affects Al extraction efficiency more than the pH. In order to correct this series of experiment, the next series were carried out.

Table 4.6 - Effect of saponification percentage and D2EHPA vol% on equilibrium pH.

Saponification Percentage	D2EHPA vol%	Equilibrium pH
80	10	6.3
40	20	4.0
27	30	3.5
20	40	3.1

4.5 Mn Extraction with 10 and 20 vol% D2EHPA in Kerosene

For the next series of experiments, two D2EHPA concentrations were chosen, 10 and 20 vol%, since the goal is to limit the co-extraction of other ions with Mn. The organic phase was saponified with various saponification percentages. L3 was elected as the aqueous feed since it has the highest Mn concentration. Fig. 4.10 demonstrates when equilibrium pH increases, D2EHPA loading percentage increases. When the equilibrium pH increased, the extraction efficiency for all the presented metal ions in the aqueous feed increased. Therefore, more moles of metal ions were transferred to the organic phase, and the D2EHPA loading percentage was increased. When the concentration of D2EHPA is lower, the loading percentage at the same equilibrium pH is higher. As mentioned previously, in order to fully load D2EHPA, the concentration of the extractant should be decreased. D2EHPA is mainly loaded with Mn in lower equilibrium pH, while in higher equilibrium pH, it is loaded with other elements that co-extracted with Mn. It is better to keep the

equilibrium pH fairly low to have a high Mn recovery with limited co-extraction of other metal ions.

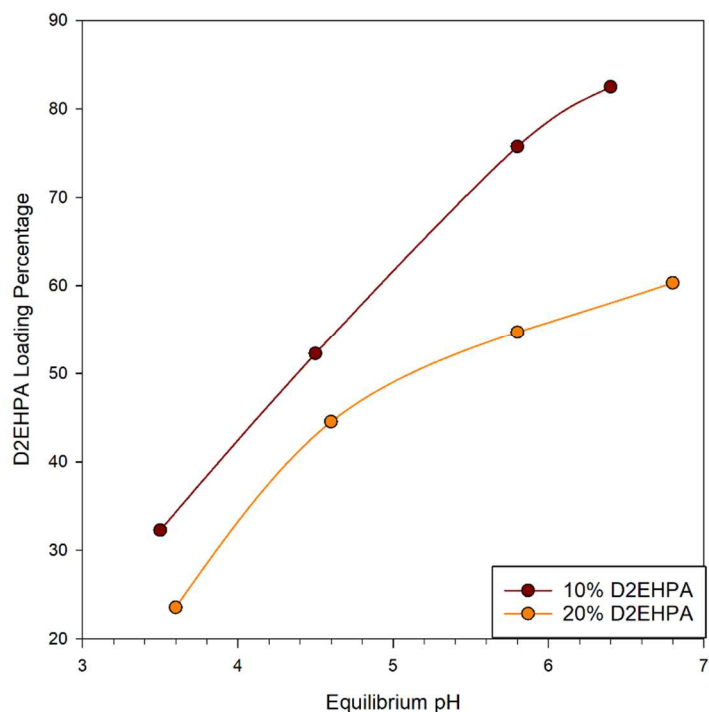


Figure 4.11 - Effect of equilibrium pH and D2EHPA concentration on D2EHPA loading percentage.

Fig. 4.12 represents the effect of saponification percentage on the $E\%$. Since the aqueous phase's pH was adjusted to 5.5, changing the saponification percentage will change the equilibrium pH. For both Co and Ni, the $E\%$ increased with the saponification percentage since higher saponification percentages mean higher equilibrium pH. As discussed before, $E\%$ of Co and Ni increases with equilibrium pH. Also, for the same saponification percentage, a higher concentration of D2EHPA leads to a rise in $E\%$ since more molecules of D2EHPA are available for extracting Co and Ni. $E\%$ of efficiency of Co is always higher than Ni because D2EHPA has more affinity towards Co [21].

$E\%$ of Mn is always close to 100% for 20 vol% D2EHPA no matter the saponification percentage since Mn can extract at equilibrium $pH < 3$. Therefore, an additional increase in saponification percentage does not have a significant effect on Mn extraction efficiency. When D2EHPA concentration decreased to 10 vol%, $E\%$ of Mn increased from 20 to 40% saponification. However,

after that, E% dropped, which could be due to the crowding effect of Co: E% of Co increased in higher equilibrium pH. Therefore, there are fewer D2EHPA molecules available to extract Mn entirely from the aqueous phase. This situation will happen when the concentration of D2EHPA is low and Co and Mn have a similar concentration in the aqueous phase.

E% of Li increased with the saponification percentage, and the changes for 20 vol% D2EHPA were more visible. When D2EHPA concentration is low, it is saturated with other metal ions that extracted prior to Li. Therefore increase in saponification percentage does not affect E% of Li.

Al extraction efficiency remained the same till 60% saponification, and then it increased. No clear correlation between pH and E% of Al was found and the reason is not clear. E% of Al increases with D2EHPA concentration since more molecules of D2EHPA are available for extraction. Cu has similar behavior to Mn, and same as Mn, the E% dropped from 40 to 60% saponification due to Co crowding effect.

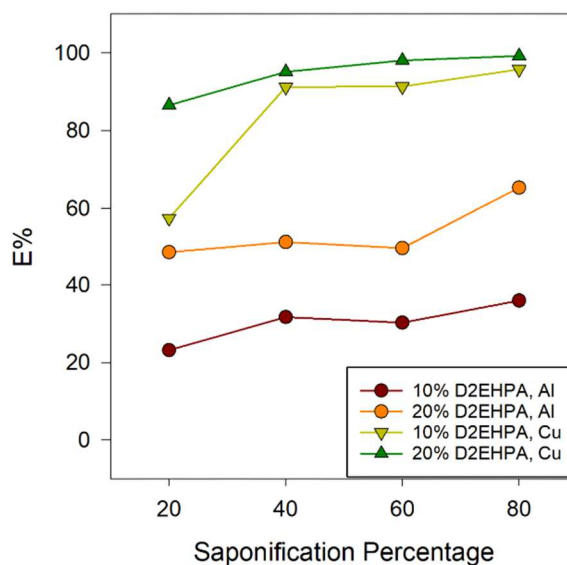
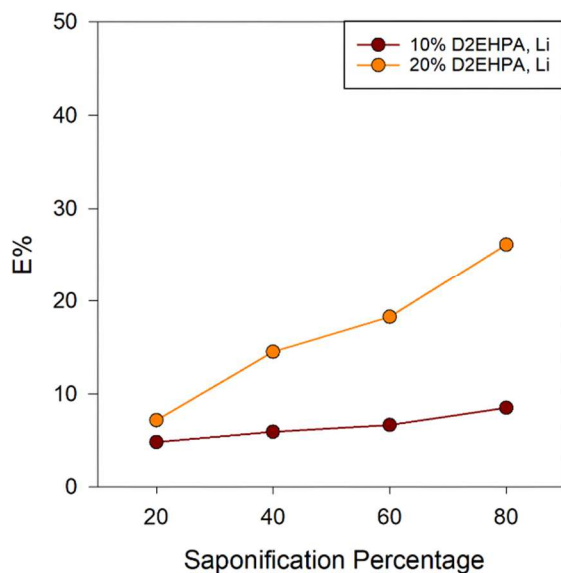
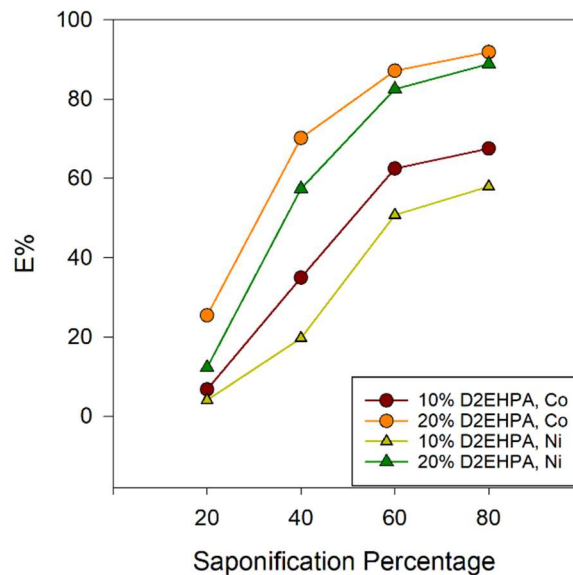
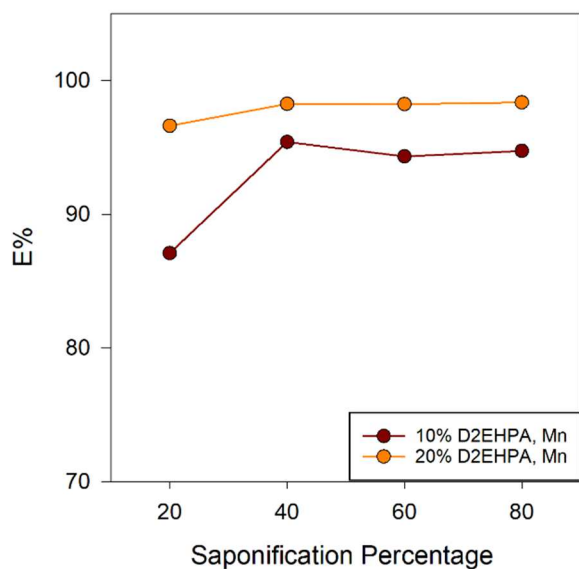


Figure 4.12 - Effect of saponification percentage on the E% of each element with various D2EHPA concentration.

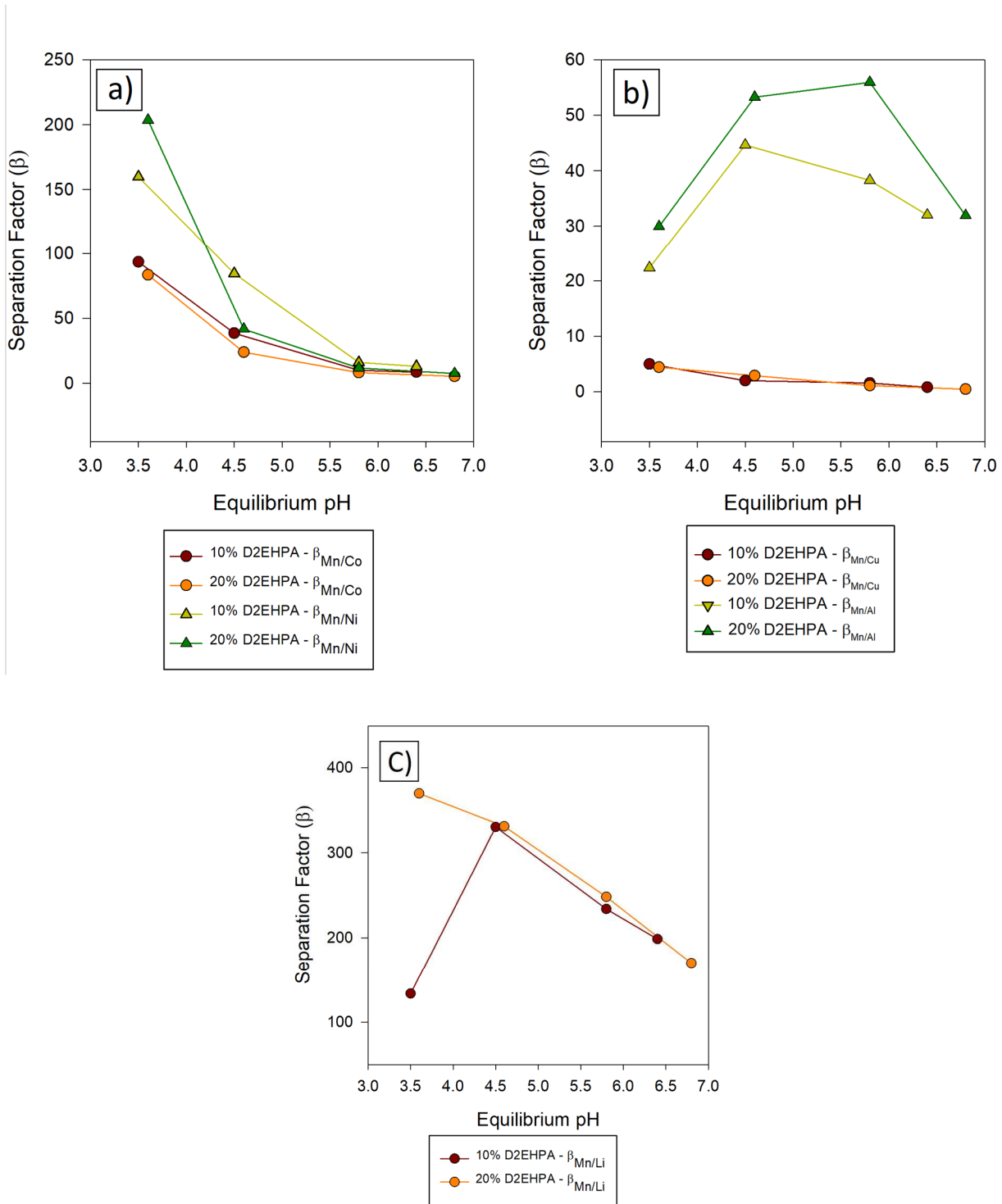


Figure 4.13 - the separation factor of Mn over other elements in different equilibrium pH, a) separation factor Mn over Co and Ni, b) separation factor of Mn over Cu and Al, c) separation factor of Mn over Li.

Fig. 4.13 exhibits the separation factor of Mn over other elements in different equilibrium pH. The separation factor was calculated based on Equation (2.7) in Ch. 2. $\beta_{\text{Mn/Co}}$ and $\beta_{\text{Mn/Ni}}$ decreased when equilibrium pH increased due to an increase in the concentration of these ions in the organic phase in higher equilibrium pH. Also, the concentration of D2EHPA affects the separation factor. For Co and Ni, in equilibrium pH > 4.5 $\beta_{\text{Mn/Co}}$ and $\beta_{\text{Mn/Ni}}$ decreased due to a higher number of D2EHPA available molecules. However, in equilibrium pH = 3.5, $\beta_{\text{Mn/Ni}}$ was higher for 20 vol% D2EHPA. Ni would not start extracting in equilibrium pH < 4, and in higher D2EHPA concentration, Mn is extracted more. For Co, the difference between $\beta_{\text{Mn/Co}}$ in 10 and 20 vol% D2EHPA is small (=10%) since Co extraction from the aqueous phase starts at equilibrium pH = 3.5.

The separation factor of Mn over Al does not follow a trend in respect to equilibrium pH. For both 10 and 20 vol% D2EHPA, $\beta_{\text{Mn/Al}}$ increased when equilibrium pH increased from 3.5 to 4.5, which could be due to an increase in Mn extraction with equilibrium pH, while for Al, the extraction did not increase since Al concentration is low. For 10 vol% D2EHPA, from equilibrium pH = 4.5 to 6.5, extraction of Mn stayed the same (due to Co crowding effect) while the extraction of Al increased. Therefore $\beta_{\text{Mn/Al}}$ decreased. For 20 vol% D2EHPA, in equilibrium pH = 5.8, extraction of both Mn and Al increased, but since D2EHPA has more affinity towards Mn, it extracts Mn more than Al; therefore, $\beta_{\text{Mn/Al}}$ increased.

When it comes to Li, $\beta_{\text{Mn/Li}}$ for 20 vol% D2EHPA decreased with equilibrium pH due to the same reasons mentioned for Co and Ni. However, for 10 vol% D2EHPA, $\beta_{\text{Mn/Li}}$ increased when equilibrium pH reached 4.5. equilibrium pH = 3.5 achieved when D2EHPA was saponified only 20%, and 80% of D2EHPA was present in the organic phase as a form of dimers rather than monomers. Since D2EHPA concentration is already low, therefore less Mn would be extracted. When saponification increased, Mn extracted more while Li extraction remained low (<6%); therefore, $\beta_{\text{Mn/Li}}$ increased. This situation is not relevant for 20 vol% D2EHPA since enough D2EHPA molecules are available for Mn extraction. $\beta_{\text{Mn/Cu}}$ is always low since both Mn and Cu have a strong affinity towards D2EHPA; Cu always co-extracts with Mn.

Based on the results presented above, the optimum condition for extracting Mn with limited co-extraction of Co, Ni, and Li is 10 vol% D2EHPA with a saponification ratio of 20%. In order to eliminate the presence of Al and Cu, it is better to adjust the pH with NaOH that is a harder base than ammonia; therefore, these two elements will precipitate before the extraction. Also, Cu can be precipitated and eliminated by adding MnS to the leachates. However, the concentration of Cu and Al is not high, and they can be eliminated with a proper scrubbing stage. Also, it is possible to remove most Mn, Cu, and Al with 20 vol% D2EHPA with a saponification ratio of 20%. Therefore, the aqueous part after extraction is enriched in Ni, Co, and Li for resynthesizing the cathode active materials. Moreover, it is possible to precipitate Co and Ni with NaOH to obtain Co and Ni products. After precipitating Ni and Co as a form of metal hydroxides, the aqueous part consists of only Na and Li. Li can be separated over Na with a β -diketone extraction system. The β -diketone extraction system will be investigated in the next chapter to separate and recover Li over Na in the wastewater, which mainly consists of Na and Li.

4.6 Extraction of Li from Wastewater using HBTA+TOPO

The elemental composition of the wastewater was determined by MP-AES. Table (4.7) demonstrates the composition of wastewater. During wet-crushing of LIBs, some of the Cu, Ni, Co, Mn and Al from the cathodes and foils were leached by water. Therefore, Cu is present in the wastewater. It is better to reduce Cu as much as possible to eliminate the co-extraction of Cu with Li. As mentioned in Chapter 2: Theory and Literature Review, pH values of the aqueous feed plays an important rule when it comes to extraction with β -diketones extractants, β -diketones are acidic extractant and their extraction ability increased by pH. In addition, increasing pH will eliminate the presence of impurities such as Cu, Ni, Co, Mn and Al. Adding NaOH drop by drop adjusted the wastewater pH to 9.5, and then the solution was filtered to obtain a precipitate-free solution. The elemental composition of wastewater after adjusting the pH can be found in Table (4.7). Wastewater at pH=9.5 was up-concentrated to investigate the effect of Li concentration on E%. After up-concentration, Na concentration was higher than MP-AES limits; therefore, some uncertainty should be considered for measuring high amounts of Na with MP-AES.

Table 4.7 - Composition of wastewater determined by MP-AES.

Element	Cu (mg/L)	Ni (mg/L)	Co (mg/L)	Li (mg/L)	Mn (mg/L)	Al (mg/L)	Na (mg/L)
Wastewater	138.46	17.45	12.59	520.82	31.32	61.85	10.66
Wastewater pH=9.5	3.86	0	0	518.33	0	0	1722.48
Wastewater up- concentrated	12.02	0	0	1145.58	0	0	6367.54

Saponification of the organic phase is needed to meet the strict pH requirement for the β -diketones extraction system [46]. HBTA was saponified by adding a calculated amount of NaOH. Saponification reaction is demonstrated below [6].



Where RH and RNa were representing HBTA and saponified HBTA, respectively.

The organic phase was consist of 0.4 M saponified HBTA and 0.4 M TOPO [6]. Previous studies [46][47][48] demonstrate that Li extraction efficiency increased when a chelating extractant was mixed with a neutral extractant. TOPO is a neural extractant, and it can extract neither Li nor Na; therefore, TOPO is a synergist to HBTA.

For the experiments, up-concentrated wastewater diluted 2 and 5 times to study different Li concentration effects. Each experiment repeated 3 times. Fig. 4.14 demonstrates the effect of Li concentration on E%.

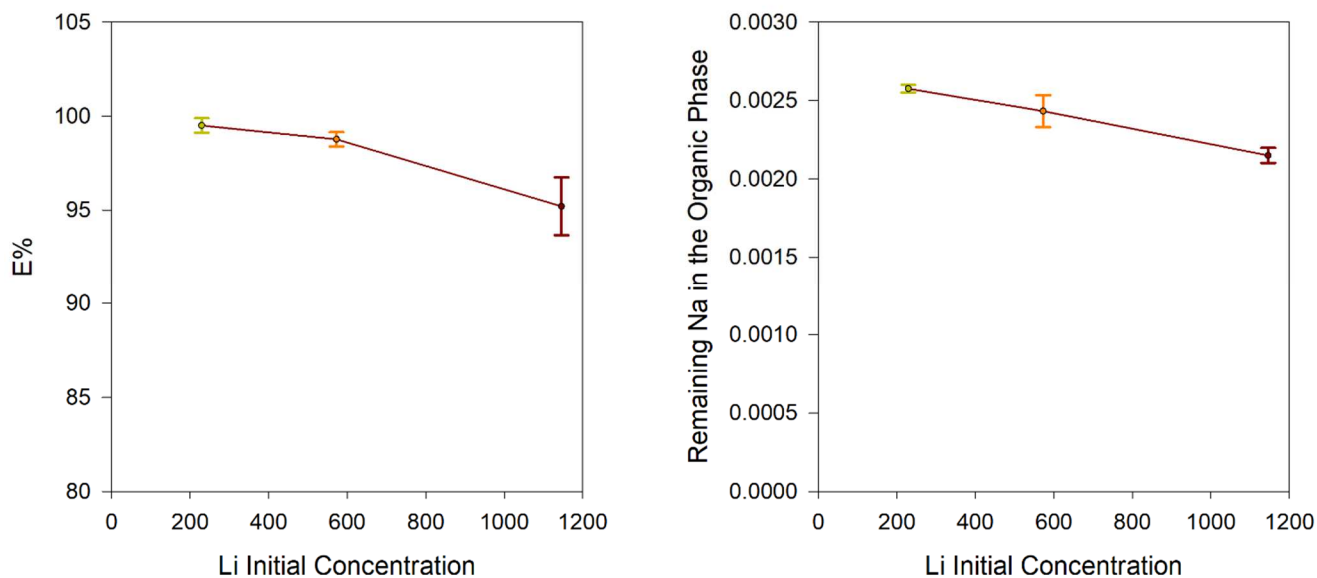


Figure 4.14 - a) E% as a function Li initial concentration, b) Remaining Na in the organic phase as Li initial concentration.

Li extraction efficiency for all the 3 different concentrations was 93% and above. Those results proved that the mixture of chelating and neutral extractant is suitable for highly efficient Li recovery from the wastewater. Li extracted from the wastewater by forming a chelate with HBTA, and chelate will form due to the interaction between Li^+ and O in the HBTA chemical structure and formation of Li-O bonds. The following reaction shows the extraction pattern [6].



The reaction above can be explained by hard and soft acid and based (HSAB). Based on HSAB theory, HBTA is considered a hard base due to the presence of F in its structure. At the same time, both Na^+ and Li^+ are regarded as hard acids [49]. However, the hardness of Li^+ (35.1 eV) is higher than the hardness of Na^+ (21.1 eV); therefore, Li^+ is harder acid than Na^+ . Based on HSAB theory, hard acids prefer hard bases, and since the difference in hardness of Li^+ and HBTA is higher than Na^+ and HBTA, it is easier for Li^+ to form a chelate with HBTA. In simpler words, HBTA has a higher affinity towards Li^+ than Na^+ . Also, Li^+ has a smaller radius than Na^+ ; therefore, the Li-O bond in the chelate is shorter than Na-O. Hence, Li-O is stronger, and the chelate formed by Li is more stable [6].

Based on Reaction (4.3), some of Na from the organic phase was transferred to the aqueous part after extraction. Therefore, all the aqueous phases after extraction have higher Na content than they have before. Fig. 4.14 represents the amount of Na that remained in the organic phase as a function of Li's initial concentration. It is clear that when the initial Li concentration decreased, the remaining Na in the organic phase increased. When Li concentration is low, there are not enough Li available to replace all the Na in the organic phase. A lower concentration of Li can cause problems during the scrubbing stage since more Na is available in the organic phase. Hence, more stages of scrubbing are needed to eliminate the presence of Na in the organic phase.

Although a lower concentration of Li can cause issues during scrubbing, up-concentration of the wastewater needs high energy usage. Therefore, the next series of experiments were done on the wastewater without up-concentration. Table (4.8) demonstrates the results for the experiments.

Table 4.8 - E% of Li from wastewater without up-concentration.

Element	Li	Cu	Na
E%	99.55	100	x
Standard Deviation	0.009	0	x
Remaining Na in the Aqueous Phase	x	x	0.002348

Based on the result presented above, it is better to lower the HBTA concentration for Li extraction from the wastewater since Li concentration is relatively low compared to previous studies [6][46]. Overall, these experiments aimed to extract Li⁺ from wastewater successfully, and that is achievable by the mixture of HBTA and TOPO.

5 Future Work:

Some future work could be further performed in this recycling route:

- Study and investigate the scrubbing and the stripping stage for loaded D2EHPA to recover Mn as MnO. MnO can be used as a lithium-ion sieve for future uses for Li recovery.
- Adding NaOH to the aqueous phase after separation from loaded D2EHPA to precipitate Ni and Co. After Co and Ni precipitation, the remaining solution is rich in Na and Li; therefore, HBTA+TOPO can be used for Li recovery, see Fig 5.1.

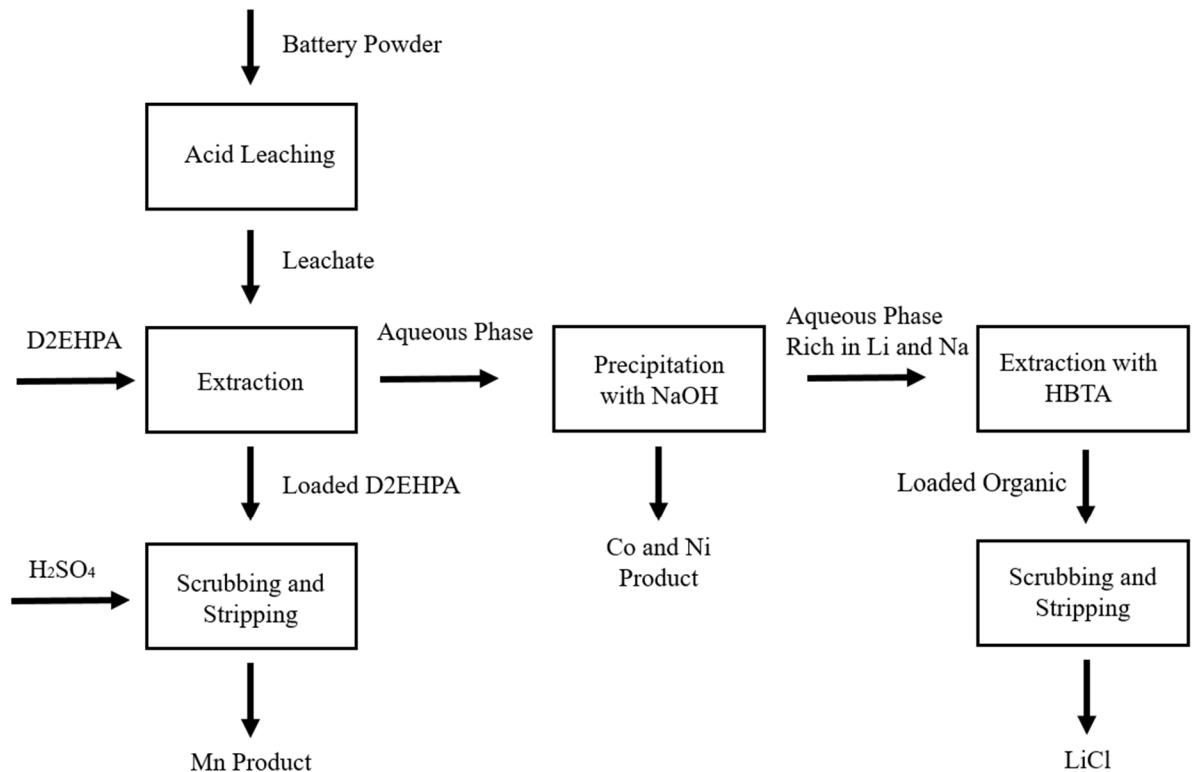


Figure 5.1 - The recommended flow diagram for LIBs recycling.

- Study the scrubbing and the stripping stage of loaded HBTA with HCl [6], to obtain LiCl as a product; see Fig 5.2.

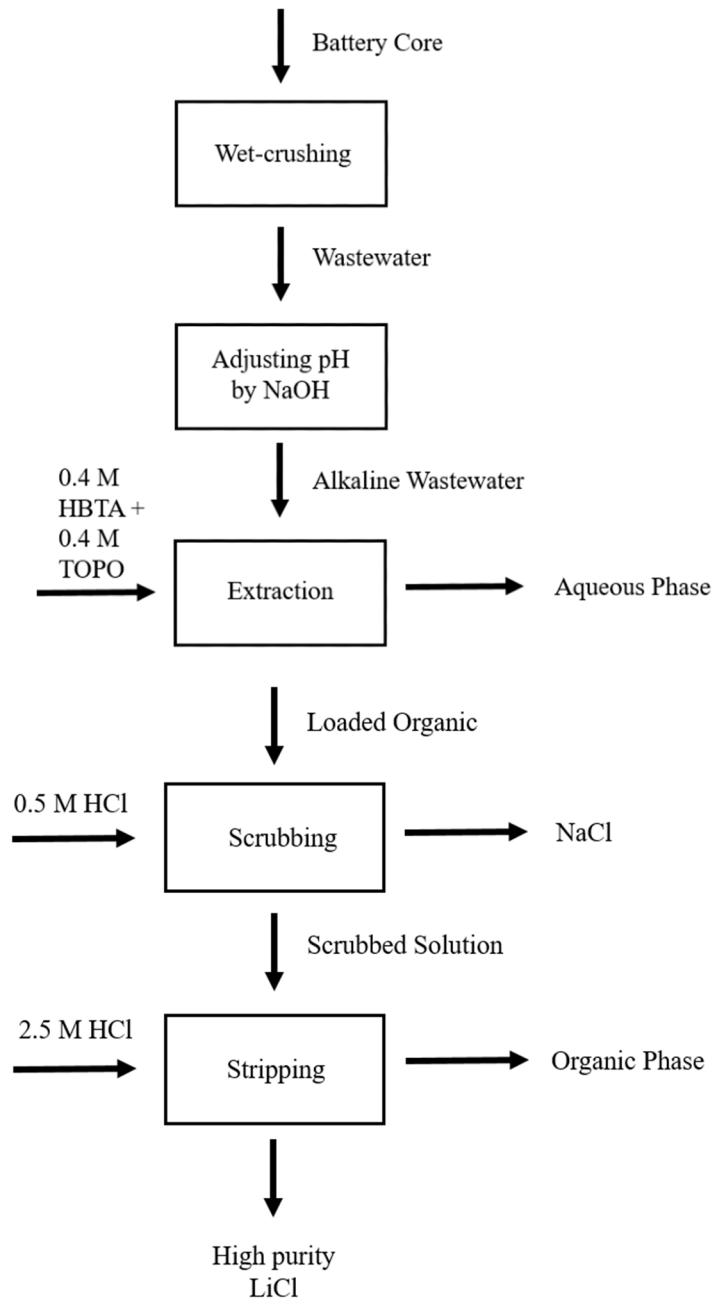


Figure 5.2 - Flow diagram for Li recycling from the wastewater.

- Using continuous or semi-continuous set-up, such as mixer-settlers for solvent extraction using HBTA+TOPO.

6 Conclusion

In this project, solvent extraction for the recovery and separation of valuable metals from spent LIBs was studied. D2EHPA (a cationic extractant) was used to study the extraction behavior of Mn, Ni, Co, Cu, and Li from an acidic sulfate media (leachates). After preliminary studies on synthetic solutions, it was clear that equilibrium pH, D2EHPA concentration, and initial concentration of metal ions in the feed solution could affect the extraction efficiency. In order to study the effect of the initial concentration of metal ions and equilibrium pH, the experiments were carried out using 40 vol% D2EHPA. The E% of Co, Ni, and Li decreased when their concentration increased in the leachates. However, the E% of Mn was always high (>90%) no matter the Mn concentration in the leachates. Also, it was found out that Cu always co-extract with Mn since D2EHPA has a high affinity for both Mn and Cu.

E% of all the elements, except Mn, increased with equilibrium pH. E% of Mn was always high throughout all the equilibrium pH (ranging from 2.1 to 6.3). In high equilibrium pH (>4), D2EHPA loses its selectivity and all the elements co-extract with each other. It was clear that D2EHPA is more selective towards Mn; therefore, selective extraction of Mn from the leachates was studied. In order to limit the co-extraction of Co, Ni, and Li, a lower concentration of D2EHPA is needed. D2EHPA can selectively extract manganese from the leachate with limited co-extraction of other cobalt, nickel, and lithium. With 10 vol% D2EHPA at the equilibrium pH of 3.5 and O/A=1, close to 90% of Mn was extracted with less than 7% co-extraction of Ni, Co, and Li. Cu and Al co-extracted with Mn, their concentration is not high in the organic phase (<130 ppm), and they can be eliminated with a proper scrubbing stage. Also, it is possible to remove most Mn, Cu, and Al with 20 vol% D2EHPA with a saponification ratio of 20%. Therefore, the aqueous part after extraction is enriched in Ni, Co, and Li for resynthesizing the cathode active materials.

Extraction of Li from wastewater of wet-crushing of spent LIBs using a combination of chelating (HBTA) and neutral (TOPO) extractant was studied. It was revealed that the HBTA+TOPO system could extract Li from wastewater with an E% of 93% and higher. Also, in the end, some future opportunities for future research were suggested.

7 Bibliography

- [1] Y. Yao, M. Zhu, Z. Zhao, B. Tong, Y. Fan, and Z. Hua, “Hydrometallurgical Processes for Recycling Spent Lithium-Ion Batteries: A Critical Review,” *ACS Sustain. Chem. Eng.*, vol. 6, no. 11, pp. 13611–13627, 2018.
- [2] J. Xu, H. R. Thomas, R. W. Francis, K. R. Lum, J. Wang, and B. Liang, “A review of processes and technologies for the recycling of lithium-ion secondary batteries,” *J. Power Sources*, vol. 177, no. 2, pp. 512–527, 2008.
- [3] G. Zubi, R. Dufo-López, M. Carvalho, and G. Pasaoglu, “The lithium-ion battery: State of the art and future perspectives,” *Renew. Sustain. Energy Rev.*, vol. 89, no. March, pp. 292–308, 2018.
- [4] S. Editors, C. Herrmann, and S. Kara, *Recycling of Lithium-Ion Batteries*. .
- [5] Z. Zhou *et al.*, “Recovery of lithium from salt-lake brines using solvent extraction with TBP as extractant and FeCl₃ as co-extraction agent,” *Hydrometallurgy*, vol. 191, no. December 2019, p. 105244, 2020.
- [6] L. Zhang *et al.*, “Lithium recovery from effluent of spent lithium battery recycling process using solvent extraction,” *J. Hazard. Mater.*, vol. 398, no. December 2019, 2020.
- [7] D. H. P. Kang, M. Chen, and O. A. Ogunseitan, “Potential environmental and human health impacts of rechargeable lithium batteries in electronic waste,” *Environ. Sci. Technol.*, vol. 47, no. 10, pp. 5495–5503, 2013.
- [8] M. Mann, A. Mayyas, and D. Steward, “Supply-Chain Analysis of Li-Ion Battery Material and Impact of Recycling,” p. 28308, 2018.
- [9] “Cobalt is critical to the renewable energy transition. How can we minimize its social and environmental cost? | Ensia.” [Online]. Available: <https://ensia.com/features/cobalt-sustainability-batteries/>. [Accessed: 03-Mar-2021].
- [10] “How Electric Cars Can Create the Biggest Disruption Since the iPhone | BloombergNEF.” [Online]. Available: <https://about.bnef.com/blog/how-electric-cars-can->

- create-the-biggest-disruption-since-iphone/. [Accessed: 03-Mar-2021].
- [11] S. Natarajan and V. Aravindan, "Recycling Strategies for Spent Li-Ion Battery Mixed Cathodes," *ACS Energy Lett.*, vol. 3, no. 9, pp. 2101–2103, 2018.
- [12] T. Georgi-Maschler, B. Friedrich, R. Weyhe, H. Heegn, and M. Rutz, "Development of a recycling process for Li-ion batteries," *J. Power Sources*, vol. 207, pp. 173–182, Jun. 2012.
- [13] L. Li *et al.*, "The Recycling of Spent Lithium-Ion Batteries: a Review of Current Processes and Technologies," *Electrochem. Energy Rev.*, vol. 1, no. 4, pp. 461–482, 2018.
- [14] J. Li, G. Wang, and Z. Xu, "Generation and detection of metal ions and volatile organic compounds (VOCs) emissions from the pretreatment processes for recycling spent lithium-ion batteries," *Waste Manag.*, vol. 52, pp. 221–227, 2016.
- [15] J. Ordoñez, E. J. Gago, and A. Girard, "Processes and technologies for the recycling and recovery of spent lithium-ion batteries," *Renew. Sustain. Energy Rev.*, vol. 60, pp. 195–205, 2016.
- [16] "The Periodic Table of Endangered Elements - American Chemical Society." [Online]. Available: <https://www.acs.org/content/acs/en/greenchemistry/research-innovation/endangered-elements.html>. [Accessed: 03-Mar-2021].
- [17] "REGULATION OF THE EUROPEAN PARLIAMENT AND OF THE COUNCIL concerning batteries and waste batteries, repealing Directive 2006/66/EC and amending Regulation (EU) No 2019/1020," Brussels, 2020.
- [18] P. Meshram, B. D. Pandey, and T. R. Mankhand, "Recovery of valuable metals from cathodic active material of spent lithium ion batteries: Leaching and kinetic aspects," *Waste Manag.*, vol. 45, pp. 306–313, 2015.
- [19] T Havlik, *Hydrometallurgy: Principles and Applications*. 2008.
- [20] C. K. Gupta and T. K. Mukherjee, *Hydrometallurgy in Extraction Processes*. 2019.
- [21] K. C. Sole, "The Evolution of Cobalt–Nickel Separation and Purification Technologies: Fifty Years of Solvent Extraction and Ion Exchange," 2018, pp. 1167–1191.

- [22] J. Li, X. Yang, Y. Fu, H. Huang, Z. Zhong, and Y. Wang, "Recovery of Fe, Mn, Ni and Co in sulfuric acid leaching liquor of spent lithium ion batteries for synthesis of lithium ion-sieve and $\text{Ni}_x\text{Co}_y\text{Mn}_{1-x-y}(\text{OH})_2$," *Hydrometallurgy*, vol. 190, no. June, p. 105190, 2019.
- [23] "4,4,4-Trifluoro-1-phenyl-1,3-butanedione 99 % | 326-06-7 | Sigma-Aldrich." [Online]. Available:
<https://www.sigmaaldrich.com/catalog/product/aldrich/217042?lang=en®ion=NO>.
 [Accessed: 03-Mar-2021].
- [24] "Trihexyltetradecylphosphonium bis(2,4,4-trimethylpentyl)phosphinate ≥ 90.0 % | 465527-59-7 | Sigma-Aldrich." [Online]. Available:
https://www.sigmaaldrich.com/catalog/product/aldrich/28612?lang=en®ion=NO&gclid=EAIaIQobChMI0Zm6vP-T7wIVQ_ iyCh0sMgTCEAAAYASAAEgL0q_D_BwE.
 [Accessed: 03-Mar-2021].
- [25] "Bis(2-ethylhexyl) phosphate 97 % | 298-07-7 | Sigma-Aldrich." [Online]. Available:
<https://www.sigmaaldrich.com/catalog/product/aldrich/237825?lang=en®ion=NO>.
 [Accessed: 03-Mar-2021].
- [26] "5137-55-3 CAS | ALIQUAT 336 | Quaternary Ammonium Compounds | Article No. 00838." [Online]. Available: <https://www.lobachemie.com/Quaternary-Ammonium-Compounds-00838/aliquat-336-CASNO-5137-55-3.aspx>. [Accessed: 03-Mar-2021].
- [27] "Trioctylphosphine oxide ReagentPlus®, 99 % | 78-50-2 | Sigma-Aldrich." [Online]. Available:
https://www.sigmaaldrich.com/catalog/product/aldrich/223301?lang=en®ion=NO&gclid=CjwKCAiA-f78BRBbEiwATKRRBN0F71cWh7vKE9AbGewbISeKhNxXWcyosO4W45zi87a-WEI0dKmYZhoCMYkQAvD_BwE. [Accessed: 03-Mar-2021].
- [28] "Tributyl phosphate | Sigma-Aldrich." [Online]. Available:
https://www.sigmaaldrich.com/catalog/substance/tributylphosphate2663112673811?lang=en®ion=NO&gclid=EAIaIQobChMI8cavp_-T7wIVkamyCh2IjQqLEAAYASAAEgJ3wPD_BwE. [Accessed: 03-Mar-2021].

- [29] K. Sarangi, B. R. Reddy, and R. P. Das, "Extraction studies of cobalt (II) and nickel (II) from chloride solutions using Na-Cyanex 272. Separation of Co(II)/Ni(II) by the sodium salts of D2EHPA, PC88A and Cyanex 272 and their mixtures," *Hydrometallurgy*, vol. 52, no. 3, pp. 253–265, 1999.
- [30] B. Swain, J. Jeong, J. chun Lee, G. H. Lee, and J. S. Sohn, "Hydrometallurgical process for recovery of cobalt from waste cathodic active material generated during manufacturing of lithium ion batteries," *J. Power Sources*, vol. 167, no. 2, pp. 536–544, 2007.
- [31] F. Wang, R. Sun, J. Xu, Z. Chen, and M. Kang, "Recovery of cobalt from spent lithium ion batteries using sulphuric acid leaching followed by solid-liquid separation and solvent extraction," *RSC Adv.*, vol. 6, no. 88, pp. 85303–85311, 2016.
- [32] F. Hu, B. P. Wilson, B. Han, J. Zhang, M. Louhi-Kultanen, and M. Lundström, "High Purity Nickel Recovery from an Industrial Sidestream Using Concentration and Liquid–Liquid Extraction Techniques," *Jom*, vol. 72, no. 2, pp. 831–838, 2020.
- [33] Y. Song, Z. Zhao, and L. He, "Lithium recovery from Li₃PO₄ leaching liquor: Solvent extraction mechanism of saponified D2EHPA system," *Sep. Purif. Technol.*, vol. 249, no. March, p. 117161, 2020.
- [34] Z. W. Chen, W. M. Gibson, and H. Huang, "High Definition X-Ray Fluorescence: Principles and Techniques," *X-Ray Opt. Instrum.*, vol. 2008, pp. 1–10, 2008.
- [35] "Supermini200 | Rigaku Global Website." [Online]. Available: <https://www.rigaku.com/products/wdxf/supermini200>. [Accessed: 03-Mar-2021].
- [36] A. F. Lagalante, "Atomic emission spectroscopy: A tutorial review," *Appl. Spectrosc. Rev.*, vol. 34, no. 3, pp. 191–207, 2004.
- [37] "MP-AES Instrument, Microwave Plasma, Agilent 4210 MP-AES | Agilent." [Online]. Available: <https://www.agilent.com/en/product/atomic-spectroscopy/microwave-plasma-atomic-emission-spectroscopy-mp-aes/mp-aes-instruments/4210-mp-aes>. [Accessed: 03-Mar-2021].
- [38] S. H. Chang, T. T. Teng, and N. Ismail, "Efficiency, stoichiometry and structural studies of Cu(II) removal from aqueous solutions using di-2-ethylhexylphosphoric acid and

- tributylphosphate diluted in soybean oil,” *Chem. Eng. J.*, vol. 166, no. 1, pp. 249–255, 2011.
- [39] P. Amani, J. Asadi, E. Mohammadi, S. Akhgar, and M. Esmaili, “Cooperative influence of D2EHPA and TBP on the reactive extraction of cobalt from sulfuric acid leach solution in a horizontal semi-industrial column,” *J. Environ. Chem. Eng.*, vol. 5, no. 5, pp. 4716–4727, 2017.
- [40] M. Manousakas *et al.*, “XRF characterization and source apportionment of PM10 samples collected in a coastal city,” *X-Ray Spectrom.*, vol. 47, no. 3, pp. 190–200, 2018.
- [41] H. Nadimi, A. Amirjani, D. H. Fatmehsari, S. Firoozi, and A. Azadmehr, “Effect of tartrate ion on extraction behavior of Ni and Co via D2EHPA in sulfate media,” *Miner. Eng.*, vol. 69, pp. 177–184, 2014.
- [42] D. Haghshenas Fatmehsari, D. Darvishi, S. Etemadi, A. R. Eivazi Hollagh, E. Keshavarz Alamdari, and A. A. Salardini, “Interaction between TBP and D2EHPA during Zn, Cd, Mn, Cu, Co and Ni solvent extraction: A thermodynamic and empirical approach,” *Hydrometallurgy*, vol. 98, no. 1–2, pp. 143–147, 2009.
- [43] N. B. Devi, K. C. Nathsarma, and V. Chakravorty, “Separation of divalent manganese and cobalt ions from sulphate solutions using sodium salts of D2EHPA, PC 88A and Cyanex 272,” *Hydrometallurgy*, vol. 54, no. 2, pp. 117–131, 2000.
- [44] R. Zhongqi, Z. Weidong, M. Huilin, L. YiMing, and D. Yuan, “Extraction equilibria of copper(II) with D2EHPA in kerosene from aqueous solutions in acetate buffer media,” *J. Chem. Eng. Data*, vol. 52, no. 2, pp. 438–441, 2007.
- [45] M. JW, *Crystallization*. 2001.
- [46] L. Zhang, L. Li, D. Shi, J. Li, X. Peng, and F. Nie, “Selective extraction of lithium from alkaline brine using HBTA-TOPO synergistic extraction system,” *Sep. Purif. Technol.*, vol. 188, pp. 167–173, 2017.
- [47] K. Ishimori, H. Imura, and K. Ohashi, “Effect of 1,10-phenanthroline on the extraction and separation of lithium(I), sodium(I) and potassium(I) with thenoyltrifluoroacetone,” *Anal. Chim. Acta*, vol. 454, no. 2, pp. 241–247, 2002.

- [48] J. Jandová, P. Dvořák, and H. N. Vu, "Processing of zinnwaldite waste to obtain Li_2CO_3 ," *Hydrometallurgy*, vol. 103, no. 1–4, pp. 12–18, 2010.
- [49] R. G. Parr and R. G. Pearson, "Absolute Hardness: Companion Parameter to Absolute Electronegativity," *J. Am. Chem. Soc.*, vol. 105, no. 26, pp. 7512–7516, 1983.

Appendix A

Calculations and MP-AES results for Ch. 4.2 are presented here.

Element	Cu (mg/L)	Ni (mg/L)	Co (mg/L)	Mn (mg/L)
Synthetic Leachate I	237.86	1112.45	562.14	765.75
Synthetic Leachate I, AE	5.14	19.38	0.00	1.12
D	45.28	56.40	X	682.71
E%	97.84	98.26	100.00	99.85
Synthetic Leachate II	128.91	1193.96	563.35	1571.21
Synthetic Leachate II, AE	5.08	42.35	3.35	1.53
D	24.38	27.19	X	1025.93
E%	96.06	96.45	100.00	99.90
Synthetic Leachate III	849.33	1079.04	532.74	389.55
Synthetic Leachate III, AE	4.24	27.87	0	0.79
D	199.31	37.72	X	492.10
E%	99.50	97.42	100.00	99.80

Synthetic Leachate IV	204.19	532.2	287.29	706.36
Synthetic Leachate IV, AE	0.00	0.00	0.00	0.00
D	X	X	X	X
E%	100.00	100.00	100.00	100.00

For synthetic leachate I, some calculation are presented below:

$$D = \frac{[Mn]_{org}}{[Mn]_{Aq,AE}} = \frac{(765.75 - 1.12)}{1.12} = 682.71$$

$$E\%_{Mn} = \frac{100D}{D + 1} = \frac{100 * 682.71}{682.71 + 1} = 99.85$$

Appendix B

Calculation and Elemental composition obtained by MP-AES for Ch. 4.3.

Element	Cu (mg/L)	Ni (mg/L)	Co (mg/L)	Li (mg/L)	Mn (mg/L)	Al (mg/L)
S/L=95	677.75	4233.69	4257.57	1438.84	3390.23	77.12
S/L=95, AE	141.46	3238.33	2708.27	1154.51	138.03	18.31
S/L=95, x5	135.88	840.52	851.73	288.39	673.87	15.54
S/L=95, x5, AE	5.68	18.93	0.39	84.29	29.30	0.22
S/L=95, x10	67.38	433.37	425.76	143.58	340.02	7.71
S/L=95, x10, AE	1.75	10.59	0.0	18.24	1.79	0.32

$$D = \frac{[Cu]_{org}}{[Cu]_{Aq,AE}} = \frac{(677.75 - 141.46)}{141.46} = 3.79$$

The distribution coefficient (D) for other elements can be calculated as the same way as it shown above.

$$E\%_{Cu} = \frac{100D}{D + 1} = \frac{100 * 3.79}{3.79 + 1} = 79.13$$

The extraction efficiency (E%) for other elements can be calculated as the same way as it shown above.

In order to calculate the D2EHPA loading percentage, one needs to know how many moles of each element is present in the organic phase.

$$[Mn]_{org} = [Mn]_{aq,before\ extraction} - [Mn]_{aq,after\ extraction}$$

$$n_{Mn,org} = \frac{[Mn]_{org} * V (mL) * 10^{-3}}{\text{Atomic mass of Mn}}$$

$$n_{D2EHPA} = n_{Mn,org} * 2$$

Same calculations were done for other elements and the equation below was used for calculating the D2EHPA loading percentage.

$$D2EHPA \text{ loading percentage} = \frac{\sum n_{Mn,Co,Li,Cu} \cdot 2 + n_{Ni} \cdot 3}{n_{D2EHPA}}$$

For S/L=95 the calculation are presented below:

Element	Cu (mg/L)	Ni (mg/L)	Co (mg/L)	Li (mg/L)	Mn (mg/L)
Org (mg/L)	793.46	893.94	1493.06	136.31	4311.78
Org (g)	0.007935	0.008939	0.014931	0.001363	0.043118
Org (mole)	0.000125	0.000152	0.000253	0.000196	0.000785

$$D2EHPA \text{ loading percentage} = \frac{(0.000785 + 0.000196 + 0.000253) \cdot 2 + (0.000152) \cdot 3}{0.012} \cdot 100 = 26.48$$

For all the other leachates, the D2EHPA loading percentages can be calculated as it shown.

Element	Cu (mg/L)	Ni (mg/L)	Co (mg/L)	Li (mg/L)	Mn (mg/L)	Al (mg/L)
S/L=120	1045.65	5276.23	5751.56	2177.43	4670.38	130.61
S/L=120, AE	252.19	4382.29	4258.50	2041.12	358.60	41.12
D	3.15	0.20	0.35	0.07	12.02	2.18
E%	75.88	16.94	25.96	6.26	92.32	68.52
Element	Cu (mg/L)	Ni (mg/L)	Co (mg/L)	Li (mg/L)	Mn (mg/L)	Al (mg/L)
S/L=120 x5	210.68	1054.66	1163.88	437.4	933.18	25.37
S/L=120 x5, AE	12.63	75.29	34.39	202.25	4.71	0.94

D	15.68	13.01	32.84	1.16	197.13	25.99
E%	94.01	92.86	97.05	53.76	99.50	96.29

Element	Cu (mg/L)	Ni (mg/L)	Co (mg/L)	Li (mg/L)	Mn (mg/L)	Al (mg/L)
S/L=120, x10	104.57	527.62	575.16	217.74	467.04	13.06
S/L=120, x10 , AE	5.02	10.34	0.00	50.60	2.20	016
D	19.83	50.03	x	3.30	211.29	80.63
E%	95.20	98.04	100.00	76.76	99.53	98.77

Element	Cu (mg/L)	Ni (mg/L)	Co (mg/L)	Li (mg/L)	Mn (mg/L)	Al (mg/L)
S/L=95E	215.12	2401.53	2371.19	796.30	1935.72	19.82
S/L=95E, AE	10.80	1618.97	1208.04	607.06	39.21	1.42
D	18.92	0.48	0.96	0.31	48.37	12.96
E%	94.98	32.59	49.05	23.76	97.97	92.48

Element	Cu (mg/L)	Ni (mg/L)	Co (mg/L)	Li (mg/L)	Mn (mg/L)	Al (mg/L)
S/L=95E, x5	43.11	478.34	486.78	160.54	390.5	4.4
S/L=95E, x5 , AE	0.26	7.18	5.18	24.26	0.06	0.23
D	164.81	65.62	92.97	5.62	6507.33	18.13
E%	99.40	98.50	98.94	84.89	99.98	94.77

Element	Cu (mg/L)	Ni (mg/L)	Co (mg/L)	Li (mg/L)	Mn (mg/L)	Al (mg/L)
S/L=95E, x10	21.51	240.15	237.12	79.63	193.57	1.98
S/L=95E, x10 , AE	0.05	0.75	1.24	10.87	0.00	0.09
D	429.24	319.20	190.23	6.33	X	21.02
E%	99.77	99.69	99.48	86.35	100.00	95.46

Element	Cu (mg/L)	Ni (mg/L)	Co (mg/L)	Li (mg/L)	Mn (mg/L)	Al (mg/L)
S/L=120E	265.80	2875.89	2990.45	994.61	2392.75	24.16
S/L=120E, AE	15.34	1957.90	1639.47	785.31	17.11	1.32
D	16.33	0.47	0.82	0.27	138.85	17.30
E%	94.23	31.92	45.18	21.04	99.28	94.54

Element	Cu (mg/L)	Ni (mg/L)	Co (mg/L)	Li (mg/L)	Mn (mg/L)	Al (mg/L)
S/L=120E x5	54.49	595.54	604.04	210.79	478.63	4.56
S/L=120E x5, AE	0.29	5.19	3.70	41.14	0.00	0.23
D	186.90	113.75	162.25	4.12	X	18.83
E%	99.47	99.13	99.39	80.48	100.00	94.96

Element	Cu (mg/L)	Ni (mg/L)	Co (mg/L)	Li (mg/L)	Mn (mg/L)	Al (mg/L)
S/L=120E, x10	26.58	287.59	299.05	99.46	239.28	2.42

S/L=120E, x10 , AE	0.07	0.51	0.98	10.92	0.00	0.12
D	378.71	562.90	304.15	8.11	X	19.13
E%	99.74	99.82	99.67	89.02	100.00	95.03

Appendix C

Calculations and MP-AES results for Ch. 4.3.

Element	Cu (mg/L)	Ni (mg/L)	Co (mg/L)	Li (mg/L)	Mn (mg/L)	Al (mg/L)
L1, x5	422.29	1856.93	1807.24	629.31	1462.19	27.96
L1, x5, 10 vol% D2EHPA, AE	7.61	876.24	619.19	552.08	49.62	3.57
D	22.98	1.12	1.92	014	28.47	6.76
E%	95.83	52.81	65.74	12.27	96.61	87.11
L1, x5, 20 vol% D2EHPA, AE	26.52	1115.57	783.64	505.18	24.79	7.82
D	14.92	0.66	1.31	0.25	57.98	2.54
E%	93.72	39.92	56.64	19.72	98.30	71.76
L1, x5, 30 vol% D2EHPA, AE	38.08	1295.42	919.28	491.1	27.23	7.96
D	10.09	0.43	0.97	0.28	52.70	2.48
E%	90.98	30.24	49.13	21.96	98.14	71.25
L1, x5, 40 vol% D2EHPA, AE	51.89	1407.77	1057.12	493.27	36.6	6.99
D	7.14	0.32	0.71	0.28	38.95	2.96
E%	87.71	24.19	41.51	21.62	97.50	74.76

For 10% D2EHPA calculations are presented below:

$$D = \frac{[Mn]_{org}}{[Mn]_{Aq,AE}} = \frac{(1462.19 - 49.62)}{49.62} = 28.47$$

The distribution coefficient (D) for other elements can be calculated as the same way as it shown above.

$$E\%_{Mn} = \frac{100D}{D + 1} = \frac{100 * 28.47}{28.47 + 1} = 96.61$$

The extraction efficiency (E%) for other elements can be calculated as the same way as it shown above.

Element	Cu (mg/L)	Ni (mg/L)	Co (mg/L)	Li (mg/L)	Mn (mg/L)	Al (mg/L)
L2, x5	146.89	1633.01	1600.1	544.06	1285.3	60.84
L2, x5, 10 vol% D2EHPA, AE	9.86	596.51	432.64	469.71	41.1	4066
D	13.90	1.74	2.70	016	30.27	0.50
E%	93.29	63.47	72.96	13.67	96.80	33.17
L2, x5, 20 vol% D2EHPA, AE	11.72	801.89	553.72	441.44	19.62	35.31
D	11.53	1.04	1.89	023	64.51	0.72
E%	92.02	50.89	65.39	18.86	98.47	41.96
L2, x5, 30 vol% D2EHPA, AE	8.77	1016.07	715.1	413.21	17.73	27.51
D	15.75	0.61	1.24	0.32	71.49	1.21
E%	94.03	37.78	55.31	24.05	98.62	54.78
L2, x5, 40 vol% D2EHPA, AE	14.71	1168.68	879.67	411.47	25.18	17.73
D	8.99	0.40	0.82	0.32	50.04	2.43
E%	89.99	28.43	45.02	24.37	98.04	70.86

For 10% D2EHPA calculations are presented below:

$$D = \frac{[Mn]_{org}}{[Mn]_{Aq,AE}} = \frac{(1285.3 - 41.1)}{41.1} = 30.27$$

The distribution coefficient (D) for other elements can be calculated as the same way as it shown above.

$$E\%_{Mn} = \frac{100D}{D + 1} = \frac{100 * 30.27}{30.27 + 1} = 96.80$$

The extraction efficiency (E%) for other elements can be calculated as the same way as it shown above.

Element	Cu (mg/L)	Ni (mg/L)	Co (mg/L)	Li (mg/L)	Mn (mg/L)	Al (mg/L)
L3, x5	221.74	2758.24	2739.58	891.43	2160.07	106.43
L3, x5, 10v ol% D2EHPA, AE	9.38	1159.81	889.77	815.63	113.62	68.11
D	22.64	1.38	2.08	0.09	18.01	0.56
E%	95.77	57.95	67.25	8.50	94.74	36.00
L3, x5, 20 vol% D2EHPA, AE	10.86	1176.25	818.42	762.05	37.75	51.78
D	19.42	1.34	2.35	0.17	56.22	1.06
E%	95.10	57.36	70.13	14.51	98.25	51.35
L3, x5, 30 vol% D2EHPA, AE	18.62	1985.16	1556.83	698.26	45.79	40.63
D	10.91	0.39	0.76	0.28	46.17	1.62
E%	91.60	28.03	43.17	21.67	97.88	61.82
L3, x5, 40 vol% D2EHPA, AE	27.63	2081.54	1684.17	664.43	58.18	30.65
D	7.03	0.33	0.63	0.34	36.13	2.47
E%	87.54	24.53	38.52	25.46	97.31	71.20

For 10% D2EHPA calculations are presented below:

$$D = \frac{[Mn]_{org}}{[Mn]_{Aq,AE}} = \frac{(2160.07 - 113.62)}{113.62} = 18.01$$

The distribution coefficient (D) for other elements can be calculated as the same way as it shown above.

$$E\%_{Mn} = \frac{100D}{D + 1} = \frac{100 * 18.01}{18.01 + 1} = 94.74$$

The extraction efficiency (E%) for other elements can be calculated as the same way as it shown above.

Appendix D

Calculations and MP-AES results of Ch. 3.5.

Element	Cu (mg/L)	Ni (mg/L)	Co (mg/L)	Li (mg/L)	Mn (mg/L)	Al (mg/L)
L3, x5	221.74	2758.24	2739.58	891.43	2160.07	106.43
L3, x5, 10 vol% D2EHPA,20% Saponification ,AE	94.33	2646.57	2555.5	848.55	278.86	81.77
D	1.35	0.04	0.07	0.05	6.75	0.30
E%	57.46	4.05	6.72	4.81	87.09	23.17
L3, x5, 10 vol% D2EHPA, 40% Saponification , AE	19.46	2215.3	1782.26	838.74	99.31	72.66
D	10.39	0.25	0.54	0.06	20.75	0.46
E%	91.22	19.68	34.94	5.91	95.40	31.73
L3, x5, 10 vol% D2EHPA, 60% Saponification ,AE	19.22	1358.17	1028.29	832.22	122.5	74.19
D	10.54	1.03	1.66	0.07	16.63	0.43
E%	91.33	50.76	62.47	6.64	94.33	30.29
L3, x5, 10 vol% D2EHPA, 80% Saponification ,AE	9.38	1159.81	889.77	815.63	113.62	68.11
D	22.64	1.38	2.08	0.09	18.01	0.56
E%	95.77	57.95	67.25	8.50	94.74	36.00

In order to calculate the separation factor of Mn over other elements, the equation below was used:

$$\beta = \frac{D_{Mn}}{D_{Metal}}$$

For 10% D2EHPA with 10% saponification, calculations were done:

$$\beta_{Mn/Cu} = \frac{D_{Mn}}{D_{Cu}} = \frac{6.75}{1.35} = 4.99, \beta_{Mn/Ni} = \frac{D_{Mn}}{D_{Ni}} = \frac{6.75}{0.04} = 159.88, \beta_{Mn/Co} = \frac{D_{Mn}}{D_{Co}} = \frac{6.75}{0.07} = 93.65$$

$$\beta_{Mn/Cu} = \frac{D_{Mn}}{D_{Li}} = \frac{6.75}{0.05} = 133.50, \beta_{Mn/Cu} = \frac{D_{Mn}}{D_{Al}} = \frac{6.75}{0.30} = 22.37$$

(All the calculations were done in Excel spreadsheets) Similar calculations were done for other saponification percentages to obtain the graphs in Ch. 3.5 (Separation factor as function of equilibrium pH).

In order to calculate the loading percentage, the formula in Ch. 3.3 was used.

$$[Mn]_{org} = [Mn]_{aq,before\ extraction} - [Mn]_{aq,after\ extraction}$$

$$n_{Mn,org} = \frac{[Mn]_{org} * V (mL) * 10^{-3}}{\text{Atomic mass of Mn}}$$

$$n_{D2EHPA} = n_{Mn,org} * 2$$

Same calculations were done for other elements and the equation below was used for calculating the D2EHPA loading percentage.

$$D2EHPA\ loading\ percentage = \frac{\sum n_{Mn,Co,Li,Cu} \cdot 2 + n_{Ni} \cdot 3}{n_{D2EHPA}}$$

For 10% D2EHPA and 80% saponification, the calculations are presented below, 10 vol% D2EHPA is equal to 0.003 moles:

Element	Cu (mg/L)	Ni (mg/L)	Co (mg/L)	Li (mg/L)	Mn (mg/L)
Org (mg/L)	212.36	1598.43	1849.81	75.8	2046.45
Org (g)	0.002124	0.015984	0.018498	0.000758	0.020465
Org (mole)	3.34E-05	0.000272	0.000314	0.000109	0.000373

D2EHPA loading percentage

$$= \frac{(0.000033 + 0.000373 + 0.000314 + 0.000109) * 2 + (0.000272) * 3}{0.003} \cdot 100 = 82.50$$

Same calculation can be applied for experiments for 20 vol% D2EHPA.

Element	Cu (mg/L)	Ni (mg/L)	Co (mg/L)	Li (mg/L)	Mn (mg/L)	Al (mg/L)
L3, x5	221.74	2758.24	2739.58	891.43	2160.07	106.43
L3, x5, 20 vol% D2EHPA,20% Saponification ,AE	29.83	2419.7	2043.7	827.7	73.29	54.54
D	6.43	0.14	0.34	0.08	28.47	0.95
E%	86.55	12.27	25.40	7.15	96.61	48.76
L3, x5, 20 vol% D2EHPA, 40% Saponification , AE	10.86	1176.25	818.42	762.05	37.75	51.78
D	19.42	1.34	2.35	0.17	56.22	1.06
E%	95.10	57.36	70.13	14.51	98.25	51.35
L3, x5, 20 vol% D2EHPA, 60% Saponification ,AE	4.35	483.13	353.71	728.46	38.24	53.43
D	49.97	4.71	6.75	0.22	55.49	0.99
E%	98.04	82.48	87.09	18.28	98.23	49.80
L3, x5, 20 vol% D2EHPA, 80% Saponification ,AE	1.71	308.32	223.62	658.47	35.33	36.9
D	128.67	7.95	11.25	0.35	60.14	1.88
E%	99.23	88.82	91.84	26.13	98.36	65.33

Appendix E

Calculations for Ch. 4.6

Element	Cu (mg/L)	Li (mg/L)	Na (mg/L)
Wastewater up-concentrated	12.02	1145.58	6367.54
Aq part, AE, Repeat 1	3.88	37.08	7983.16
Aq part, AE, Repeat 2	4.02	72.37	7845.02
Aq part, AE, Repeat 3	3.51	55.16	7763.98
Wastewater up-concentrated, x2	6.01	572.79	3183.77
Aq part, AE, Repeat 1	1.73	5.10	3927.12
Aq part, AE, Repeat 2	2.01	6.68	4298.07
Aq part, AE, Repeat 3	1.05	9.41	3864.30
Wastewater up-concentrated, x5	2.40	229.12	1273.51
Aq part, AE, Repeat 1	0.00	0.28	1726.36
Aq part, AE, Repeat 2	0.00	1.09	1816.05
Aq part, AE, Repeat 3	0.00	2.05	1828.05

Distribution coefficients (D) and extraction efficiency (E%) were calculated for Li. For up-concentrated wastewater, repeat 1, calculations are presented.

$$D = \frac{[Li]_{org}}{[Li]_{Aq,AE}} = \frac{(1145.58 - 37.08)}{37.08} = 29.89, \quad E\%_{Li} = \frac{100D}{D+1} = \frac{100 \times 29.89}{29.89+1} = 96.76$$

In order to calculate remaining Na in the organic part, one need to know how much NaOH was added to the organic phase for saponification. 560 μL of NaOH is equal to 0.0028 moles of NaOH. Therefore, remaining Na can be calculated.

$$\textit{Remaining Na} = 0.0028 - \frac{(7983.16 - 6367.54) * 10^{-5}}{23} = 0.002098$$